Estimating the age and growth of yellowfin tuna (*Thunnus albacares*) in the Indian Ocean from counts of daily and annual increments in otoliths

Jessica Farley[1], Kyne Krusic-Golub[2], Paige Eveson[1], Patricia L. Luque[3], Naomi Clear[1], Igaratza Fraile[3], Iraide Artetxe-Arrate[3], Iker Zudaire[3], Annie Vidot[4], Rodney Govinden[4], Ameer Ebrahim[4], Mohamed Ahusan[5], Evgeny Romanov[6], Umair Shahid[7], Emmanuel Chassot[8,9], Nathalie Bodin[8,10], Denham Parker[11], Hilario Murua[12], Francis Marsac[13], Gorka Merino[3]

[1] CSIRO Oceans and Atmosphere, Hobart, Australia; jessica.farley@csiro.au

[2] Fish Ageing Services Pty Ltd, Victoria, Australia; kyne.krusicgolub@fishageingservices.com

[3] AZTI, Marine Research, Basque Research and Technology Alliance (BRTA), Pasaia, Gipuzkoa, Spain; gmerino@azti.es

[4] Seychelles Fishing Authority, Victoria, Seychelles; rgovinden@sfa.sc

[5] Ministry of Fisheries, Marine Resources and Agriculture, Malé, Maldives; mohamed.ahusan@gmail.com

[6] CAP RUN - CITEB (Centre technique de recherche et de valorisation des milieux aquatiques), Île de la Réunion; evgeny.romanov@ird.fr

[7] WWF Pakistan, Karachi, Pakistan; ushahid@wwf.org.pk

[8] Research Institute for Sustainable Development (IRD), Victoria, Seychelles

[9] IOTC Secretariat, Victoria, Seychelles; Emmanuel.Chassot@fao.org

[10] Sustainable Ocean Seychelles (SOS), Beau Belle, Seychelles; natbod@gmail.com

[11] South African Department of Environment, Forestry and Fisheries (DEFF), Cape Town, South Africa; denhamparker@gmail.com

[12] International Seafood Sustainability Foundation, Washington DC, USA; hmurua@iss-foundation.org

[13] Research Institute for Sustainable Development (IRD), UMR MARBEC, Victoria, Seychelles; francis.marsac@ird.fr

Executive summary

This paper describes work to estimate the age and growth of yellowfin tuna (*Thunnus albacares*) in the Indian Ocean from otoliths as part of the 'GERUNDIO' project[1]. The 2018 stock assessment for yellowfin tuna in the Indian Ocean (IOTC) indicated that the stock is

[1] Collection and analysis of biological samples of tropical tunas, swordfish, and blue shark to improve age, growth and reproduction data for the Indian Ocean Tuna Commission (IOTC), FAO Contract No. 2020/SEY/FIDTD/IOTC - CPA 345335.

overfished and subject to overfishing (Fu et al. 2018; IOTC 2020). The stock assessment model used a fixed growth function from Fonteneau (2008) in the base model and additional growth curves from Eveson et al. (2015) and Dortel et al. (2015) in sensitivity models. All of these growth models suggest growth of yellowfin tuna is slow between 30 and 60 cm fork length (FL) before changing to much faster growth between 60 and ~120 cm FL. The Fonteneau (2008) model is based on growth information from tag-recapture data collected during the Indian Ocean Tuna Tagging Programme (IOTTP), the Eveson et al. (2015) models integrate the IOTTP tag-recapture data with otolith-based daily age estimates from Sardenne et al. (2015), and the Dortel et al. (2015) models use different combinations of the tag-recapture and otolith daily age data as well as length-frequency data from the purse seine catches. The otolith-based daily age estimates from Sardenne et al. (2015) varied considerably among readers, and there was a recommendation by Sardenne et al. (2015) to explore alternate ageing methods such as annual ageing of otoliths (as opposed to daily ageing). Recently, Farley et al. (2017; 2020) developed a new method to estimate the decimal age of bigeye tuna in the western and central Pacific Ocean from validated counts of daily and annual growth zones in otoliths. The aim of the current study is to apply this method to yellowfin tuna in the Indian Ocean to obtain new estimates of age and growth, and to attempt to validate the age estimates using otoliths and data from yellowfin tuna tagged and recaptured in the IOTTP.

Otoliths from 1479 yellowfin tuna collected in the current and previous projects were available for analysis, ranging in size from 20.5 to 179 cm FL. Of these, 253 otoliths were selected for ageing. A combination of daily and annual ageing was undertaken, and a final age was obtained for 250 of the 253 fish. The youngest fish was aged 53 days and the oldest was 10.9 years. The preliminary age validation work using otoliths and data from the IOTTP provides evidence that the otolith ageing method used in this study is accurate. However, we recommend that further age validation work is undertaken, including the analysis of bomb radiocarbon (^{14}C) data from otoliths (currently underway as part of the GERUNDIO project) and analysis of the OTC marked otoliths by a reader with no prior knowledge of the time at liberty or fish length.

Four growth models were fit to the age and length data (von Bertalanffy (VB), Richards, VB log k, and 2-stage VB). All four models provided very similar fits; however, the 2-stage VB model provided a better fit to the data for fish ~<55 cm FL. The length-at-otolith weight data (which is independent of the age estimation method) showed a change in otolith growth at ~55 cm FL, which is consistent with the length-at-age data and lends support to the 2-stage VB model. Overall, our analysis shows that growth is rapid in the first few years with fish reaching ~60 cm FL at age 1 and ~95 cm FL at age 2. Mean asymptotic length was estimated to be ~163 cm FL.

The 2-stage VB growth curve estimated in the current study is similar to growth estimated by Multifan-CL (MFCL) in the 2008 stock assessment for fish ~<90 cm FL. The divergence in growth for fish larger than 90 cm FL is not surprising since MFCL relies on length frequency data from catches to estimate growth parameters, which are imprecise when length modes merge across age classes as fish grows. In contrast, our two-stage VB growth curve is quite different from the "ad hoc" growth curve of Fonteneau (2008) and VB log k growth curves of

Eveson et al. (2015) and Dortel et al. (2015). In particular, we do not see the same slow growth for fish <60 cm, followed by a rapid increase. Furthermore, we estimate mean asymptotic length to be much higher (~163 cm FL) compared to the growth curves that included tag-recapture data (130.7 cm FL in Eveson et al. 2015; ~139 cm FL in Dortel et al. 2015). This may, at least in part, be due to the low number of fish >150 cm FL in the tag-recapture data available at the time to be used in Eveson et al. (2015) and Dortel et al. (2015), which is likely related to the relatively short times at liberty of fish included in the analysis (<6 years) compared to the current estimated longevity of yellowfin tuna of at least 10 years.

We recommend that additional otoliths are collected from the northern and eastern regions of the Indian Ocean, and that these otoliths and additional otoliths from those already collected in the GERUNDIO and IOTTP projects are read/aged to provide further information on growth and longevity. These data will also be useful for assessing the potential for inter-annual variation in length at age affecting estimation of the growth curve.

1. Introduction

Yellowfin tuna (*Thunnus albacares*) is a highly migratory species that inhabits the epipelagic zone of tropical and subtropical waters of the three major oceans, from latitudes of approximately 45°N to 45°S (Collette et al. 2001). Their spawning areas are restricted to environments with warm sea surface temperatures (>20-24°C) and mesoscale oceanographic activity (Reglero et al., 2014; Schaefer, 2001). Yellowfin tuna represents an important source of nourishment and livelihood for numerous nations around the world (FAO, 2020; Guillotreau et al., 2017). It is also a significant component of the global fisheries market, being among the top 10 most fished marine species, and constitutes the second largest tuna fishery worldwide (FAO 2020; McKinney et al. 2020). As such, this species experiences significant fishing pressure, with global catches reaching about 1.45 million tonnes in 2018 (FAO 2020).

Yellowfin tuna is managed as a single stock within the Indian Ocean. Genetic studies indicate that the population structure within the Indian Ocean is complex (Kunal et al. 2013; Barth et al. 2017), and a recent study found evidence for genetic structure north and south of the equator (Grewe et al. 2020). The 2018 stock assessment for yellowfin tuna in the Indian Ocean, which considers both stock abundance and fishing mortality, indicated that the stock is overfished and subject to overfishing (Fu et al. 2018; IOTC 2020). An integral part of developing stock assessment models is to have a sound understanding of growth (Maunder and Piner, 2015; Methot and Wetzel 2013). Growth models are used in stock assessments to convert length measurements of the catch to age measurements, and to model biomass and fishing processes over time (Murua et al. 2017).

The age and growth of yellowfin tuna has been investigated widely in the Atlantic, Pacific and Indian Oceans (see review by Murua et al. 2017). Several approaches have been used to estimate the growth of yellowfin tuna in the Indian Ocean, including: (1) modal analyses of length frequencies, (2) the examination of daily and annual increments in calcified structures (e.g., otoliths and vertebrae) and (3) growth information obtained from tag and recapture data. Recent studies have generally supported a two-stanza growth curve for Indian Ocean yellowfin tuna, with a slow initial growth phase up to ~60 cm FL followed by much faster growth.

The 2018 stock assessment used an 'ad hoc' two-stanza growth curve from Fonteneau (2008) in the base model and two-stanza growth curves from Eveson et al. (2015) and Dortel et al. (2015) in sensitivity models. Fonteneau (2008) estimated growth using tag-recapture data from the Indian Ocean Tuna Tagging Programme (IOTTP; Murua et al. 2015); Eveson et al. (2015) used the IOTTP tag-recapture data along with otolith-based daily age estimates from Sardenne et al. (2015); and Dortel et al. (2015) used these same sources of information (with a more stringent selection criteria applied to the tag-recapture data) as well as modal progressions in length frequency data from the purse seine fishery collected in 2000-2010.

In 2020, the European Union and the IOTC supported the "GERUNDIO" project for the "collection and analysis of biological samples of tropical tunas, swordfish, and blue sharks to improve age, growth and reproduction data for the IOTC". The project developed a sampling scheme to collect new biological samples from across the IOTC assessment region and the analysis of new samples and existing materials from previous research initiatives. This paper provides preliminary otolith-based age and growth estimates for yellowfin tuna in the IOTC assessment region undertaken in this project. The aim was to follow methods recently developed by Farley et al. (2020) to estimate the age and growth of yellowfin tuna in the Western and Central Pacific Ocean (WCPO) from counts of daily and annual growth zones in otoliths. In addition, a priority for the project was to undertake initial age validation work for yellowfin tuna by analysing otoliths from fish that had been tagged and recaptured in the IOTTP. In addition, the project is applying bomb radiocarbon (^{14}C) age verification methods to verify the annual ageing protocols used (see Ishihara et al., 2017; Andrews et al., 2020). Otoliths from 30 yellowfin tuna were selected for analysis and the samples (whole and extracted) were submitted to the Beta Analytic Carbon Dating Service (https://www.radiocarbon.com/) for accelerator mass spectrometry (AMS) analysis to determine sample ^{14}C levels. Preliminary data has been received but data analysis has not been completed. We anticipate that additional otoliths will be analysed for to increase the sample size for the final ^{14}C analysis.

2. Methods

2.1. Sample collection and selection for ageing

Sagittal otoliths from 1479 yellowfin tuna were available for analysis (as of 1 October 2021). They were collected in the GERUNDIO project as well in the previous "*Estimation of Maternal effects On the sustainability of large pelagic populaTIONs*" (EMOTION) (Bodin et al. 2018) and "*Population Structure of Tuna, Billfish and Sharks in the Indian Ocean*" (PSTBS-IO) projects (Davies et al. 2020). The otoliths were collected between 2009 and 2021 from across the Indian Ocean. Figure 1 shows the sampling locations by area for all otoliths divided into those aged and not aged. Exact catch location is not currently available for all samples to plot a more detailed map. Straight fork length (FL) was measured to the nearest cm for all fish. Sex data was available for 807 fish.

The otoliths were cleaned, dried, and a proportion were weighed to the nearest 0.001 g if complete. Otoliths from 253 yellowfin tuna were selected for ageing based on fish length and sampling location to ensure age estimates were obtained from length classes where sample sizes were small and from across the spatial range of fish sampled. Note that 'sister' otoliths from a subset of these fish were selected for bomb radiocarbon age validation (see Introduction). Figure 2 shows the size frequency of fish selected for ageing and those remaining in the archive for future analysis.

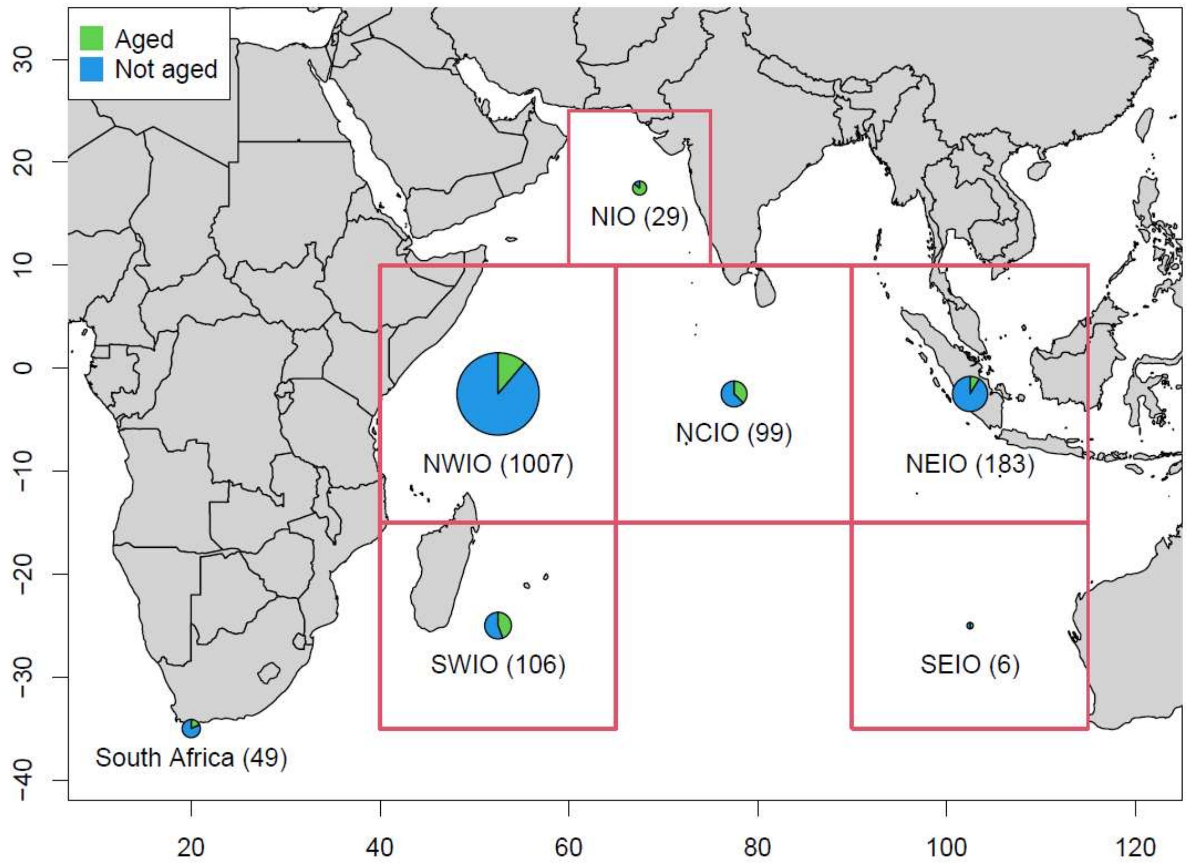

Figure 1. Map of the sampling locations for yellowfin tuna. Circle size is proportional to sample size, and colours indicate the proportion of otoliths that have been aged and are included in the growth analysis (green) and the proportion remaining in the collection for future analysis (blue). The total number of samples collected is in brackets. Longitude is shown in degrees east. NIO = north Indian Ocean, NWIO = northwest Indian Ocean, SWIO = southwest Indian Ocean, NCIO = north central Indian Ocean, NEIO = northeast Indian Ocean, SEIO = southeast Indian Ocean.

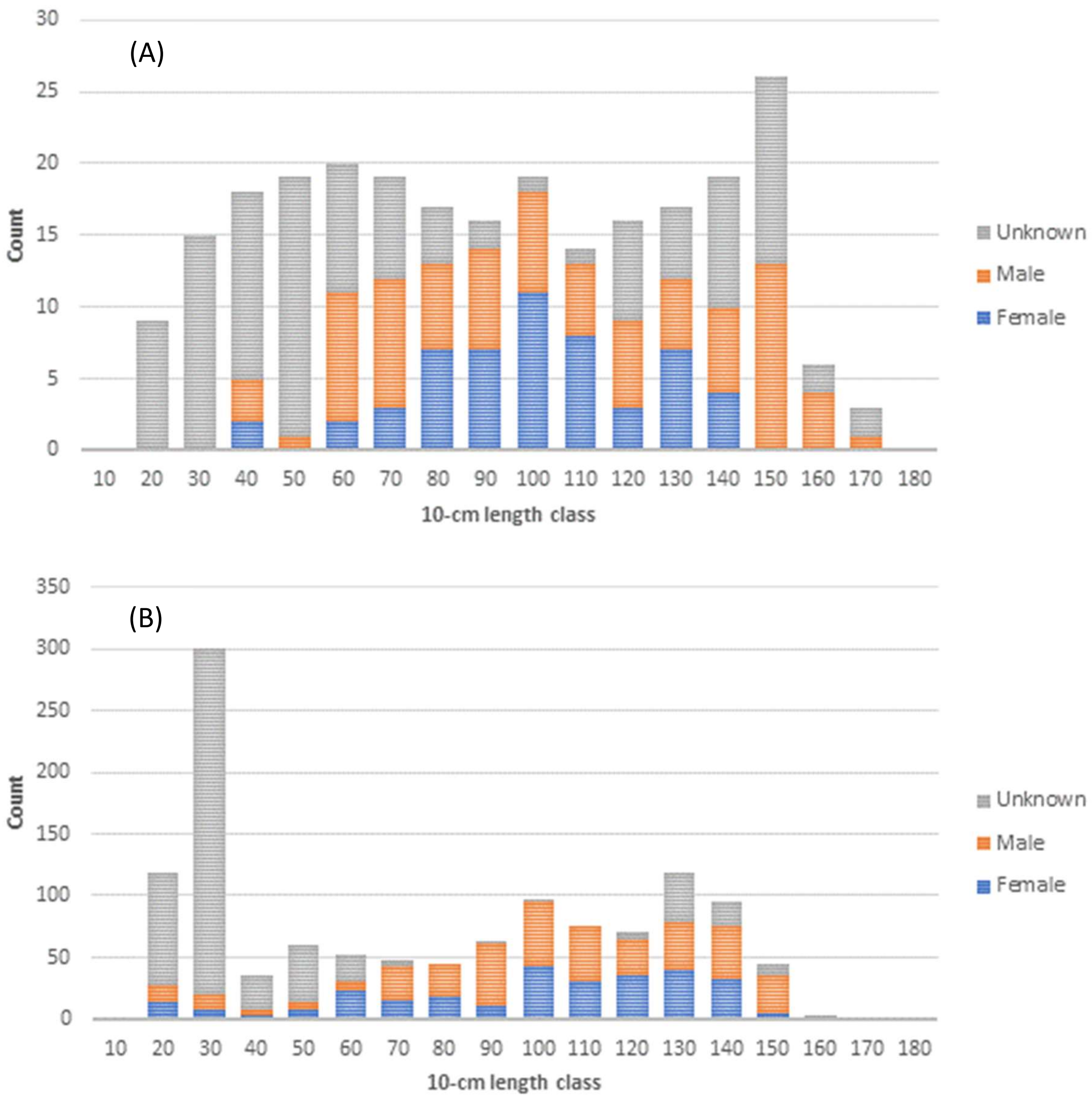

Figure 2. Length frequency (fork length) of yellowfin tuna (A) selected for ageing and included in the preliminary growth analysis for the Indian Ocean in this study (n=253), and (B) remaining in the collection from the Indian Ocean (n=1226). The lower boundary length value of the bin is shown.

2.2. Otolith preparation and reading

Both daily and annual increments were examined in this study following methods developed for yellowfin in the WCPO (Farley et al. 2017; 2020).

Daily ageing

A total of 74 samples were selected from small fish (20.5-78.5 cm FL) for preparation for daily age reading. The method involves preparing single longitudinal (frontal) sections from the primordium to the postrostral axis of the otolith, through the primordium (Williams et al.

2013). The number of visible microincrements (assumed daily growth zones) were counted from the primordium to the terminal edge of the section under high magnification on a compound microscope. All otoliths were prepared and read by Fish Ageing Services Pty Ltd (FAS) in Australia. Each sample was read twice by the same reader and if the difference in counts was >10%, then a third reading was completed. The average of the two closest readings was used as the final count.

An additional sub-sample of nine transverse sections used in the Sardenne et al. (2015) study was selected for re-reading. Microincrements were counted using a transmitted light microscope at various magnifications ranging between 400 and 1000x depending on the area of the otolith being interpreted. The reading transects in this study varied slightly from that used in the Sardenne et al. (2015) study (see Figure 3), where the first zones were counted closer to the sulcal edge where they are sequential and evenly spaced. The widely spaced zones when counted along the transect used by Sardenne et al. (2015) from the primordium to the first inflection are made up of quite a few split zones, which are difficult to interpret particularly at higher magnification.

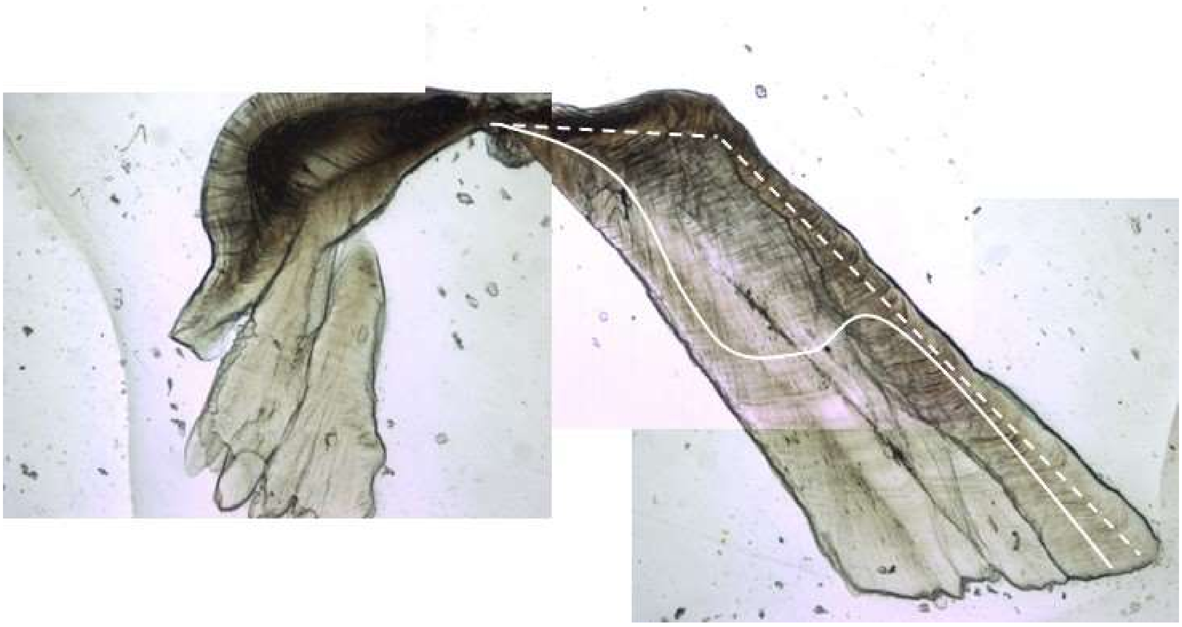

Figure 3. Image of a transversely prepared yellowfin tuna otolith section for daily age reading showing the reading path used by Sardenne et al. (2015) (dashed line) and that used in this study (solid line).

Annual ageing

A total of 203 otoliths were selected from fish ranging 51-179 cm FL for annual age reading (24 were sister otoliths of those prepared for daily age estimation above). The otoliths were prepared following the methods outlined in Anon (2002). Otoliths were embedded in clear casting polyester resin and four or five serial sections approximately 300 μm thick were cut from each otolith (around the primordium). Sections from each sample were cleaned, dried, and mounted on glass microscope slides (50 × 76 mm) with resin. Sections were then covered with further resin and two glass coverslips (22 × 60 mm) were placed side by side. All otoliths were prepared and read by FAS using a dissecting microscope and transmitted light. An image analysis system was used to read the sectioned otoliths. The system counts and measures the distance of each manually marked opaque zone (marked on the outer edge of each opaque zone) from the primordium and collects an annotated image from each sample read. The opaque zones at the terminal edge of the otolith were only marked if they were complete and some translucent material was evident after the opaque zone. The otolith edge was classified as new opaque, narrow translucent or wide translucent based on the criteria developed for Pacific yellowfin tuna otoliths (Farley et al. 2017) and each reading was assigned a confidence score of 0-5 (poor-good). All samples were read by the same reader a second time to determine intra-reader ageing error. Average percent error (Beamish and Fournier 1981) and age difference tables were used to assess the precision of readings.

Decimal age was calculated for each fish with an annual count based on the method developed for yellowfin and bigeye tuna (*Thunnus obesus*) in the western Pacific Ocean (Farley et al. 2020):

First, the age of each fish when the first opaque zone was completed in the transverse section was calculated. This was done using the relationship between daily age and otolith size for paired otoliths (Append Figure 1). Daily age estimates were obtained from the longitudinal sections (as described in previous section "Daily ageing") and otolith size was the measurement from the primordium to the distal edge of the first opaque zone on the transverse section of the 'sister' otolith prepared for annual ageing. The daily age-otolith size relationship was estimated using a power curve (Append Figure 1) as it provided the best fit to the data.

Second, the number of complete annual increments in the otolith was calculated. A complete annual increment is one opaque zone + one translucent zone, which represents one year of growth, and is calculated as the total count of opaque zones minus 1.

Third, the time elapsed after the last counted opaque zone was deposited and when the fish was caught was estimated. This was calculated using the size of the marginal increment in the otolith prepared as a proportion of the mean size of the complete annulus for that age group (see Append Figure 2). The mean increment size was calculated using the otolith measurements taken routinely for each otolith included in the annual ageing. The distance between the terminal edge of each opaque zone was calculated, and the mean size estimated for each age group.

The total age of each fish was estimated by adding together the age components estimated in each step. Note that for otoliths with zero or one opaque zones (within the range of the power curve in Append Figure 1), age was estimated using only the otolith measurement (i.e., only step 1).

2.3. Age validation and verification

Analysis of IOTTP tag-recapture otoliths

Age validation for yellowfin tuna was undertaken using otoliths from fish that had been tagged and recaptured as part of the IOTTP and were at liberty for up to 6.4 years. These otoliths were not used in the daily or annual ageing above (i.e., Section 2.2). A total of 120 otoliths were sent to FAS where they were weighed to the nearest 0.0001 g if complete.

A subset of the otoliths was selected for annual ageing by FAS, which consisted of (1) four OTC marked samples ranging from 2.23 to 2.57 years at liberty and 115 to 130 cm FL length at recapture, and (2) 14 non-OTC marked samples ranging from 1.98 to 6.31 years at liberty and 131 to 152 cm FL at recapture. Transverse sections were prepared using the same method as described in section 2.2. The only modification was that during the processing of the OTC samples, the blocks and slides were not subject to heat and were stored in a dark box while the resin cured as both heat and direct light can reduce the intensity of the OTC mark prior to examination.

Otoliths marked with OTC were examined for the presence and position of the OTC mark using a Leitz Diaplan compound microscope fitted with a 100-W incident ultraviolet light source, and a Leitz D filter block (excitation filter 450–520 nm) to suit the fluorescent properties of OTC. One image was captured of the otolith under fluorescent illumination and another under transmitted light for direct comparison.

Since the time at liberty was known for each fish (i.e., a truly blind read was not possible at this time), we used an objective method to verify the annual age estimation method used in this study. For each of the 18 sectioned otoliths, we measured the distance from the primordium to the otolith edge on the counting path. We then estimated the age of the fish at recapture by summing the estimated age of the fish when it was tagged (using its length measurement and the relationship in Figure 4 below) and the time at liberty. Only fish <70 cm FL at release were included in the analysis since this was the maximum length used in developing the length and daily age relationship based on otolith readings (Figure 4). We compared the relationship between age and the size of the sectioned otolith to the same information from the otoliths of all yellowfin tuna aged in this study, to determine if the data were consistent and provide evidence that the otolith age estimates obtained in the current study are accurate. A blind read of the OTC marked otolith will be undertaken in the future.

Analysis of IOTTP tag-recapture data

Further age validation for yellowfin tuna was undertaken using the IOTTP tag-recapture data. Using the method described above, we estimated the age at recapture for all fish recaptured, not just the 18 selected for reading in the current study (i.e., by summing the estimated age of the fish when it was tagged/released and the time at liberty). Only fish <70 cm FL at release were included in the analysis since this was the maximum length used in developing the length and daily age relationship based on otolith readings (Figure 4) for estimating age at release. The length-at-age (estimated at recapture) was compared to the length-at-age estimated for all fish aged in the study, to determine if the data were consistent providing further evidence that the annual ageing method is accurate.

2.4. Growth analysis

Four different growth models were fit to the age and length data for yellowfin tuna: (1) von Bertalanffy (1938) (VB); (2) Richards (1959); (3) VB with a logistic growth rate parameter (Laslett et al. 2002) (VB log k); and (4) 2-stage VB (similar to Hearn & Polacheck (2003) except the transition is parameterised in terms of age instead of length). Age estimates from both daily counts and from annual counts after applying the decimal age algorithm were included in the models.

The VB growth model has the form:

$$L_a = L_\infty(1 - e^{-k(a-a_0)})$$

where L_a is the fork length at age a, L_∞ is the mean asymptotic length, k is a relative growth rate parameter (year^{-1}), and a_0 is the age at which fish have a theoretical length of zero. We fit the model using maximum likelihood estimation assuming a Gaussian error structure with mean 0 and variance σ^2.

The Richards model can be expressed in different ways, but here we used the following parameterisation:

$$L_a = L_\infty(1 - {}^{1}\!/_{b}\, e^{-k(a-a^*)})^b$$

where L_∞ and k are defined as for the VB model, a^* determines the point of inflection and b governs the shape of the curve. Note that when b = 1, the Richards equation is equivalent to the VB equation.

The VB log k model has the form:

$$L_a = L_\infty \left\{ 1 - e^{-k_2(a-a_0)} \left(\frac{1 + e^{-\beta(a-a_0-\alpha)}}{1 + e^{\alpha\beta}} \right)^{-\frac{(k_2-k_1)}{\beta}} \right\}$$

where this function allows for a change in growth from a VB curve with growth rate parameter k_1 to a VB curve with growth rate parameter k_2. There is a smooth transition between the two stages governed by a logistic function, where α governs the age at which the midpoint of the transition occurs and β governs the rate of the transition (being sharper for larger values).

The 2-stage VB curve has the form:

$$L_a = \begin{cases} \gamma L_\infty(1 - exp(-k_1(a - a_0))) & \text{for } a \le \alpha \\ L_\infty(1 - exp(-k_2(a - a_0 - \tau))) & \text{for } a > \alpha \end{cases}$$

where $\tau = \alpha + \frac{1}{k_2}\log\left(1-\gamma(1-\exp(-k_1\alpha))\right)$.

This equation represents a VB curve with growth rate parameter k_1 and asymptotic length γL_∞ up to age α, then a VB curve with growth rate parameter k_2 and asymptotic length L_∞ after age α. The term τ is necessary to ensure the two curves match up at the change-point α. Note that the 2-stage VB model differs from the VB log k model in that it allows for a different L_∞ in the first growth phase. A possible disadvantage is that it has an abrupt switch between the two VB curves at age α, whereas the VB log k allows for a slower transition (through the β parameter).

To fit these models, we used maximum likelihood estimation assuming a Gaussian error structure with mean 0 and variance σ^2. Akaike's information criterion (AIC) (Akaike 1974) and plots of residuals were used to compare the fits.

3. Results

3.1. Daily ageing

Age estimates were obtained from all 74 otoliths selected for daily ageing. For 53 otoliths, the first two reads were within 10%, so the age estimate was the average of these two reads. For the remaining 21, a third read was required and the average of the closest two reads was taken. Age ranged from 53 to 542 days (Figure 4). Generally, the microincrement pattern along the preferred reading path (Figure 5) was relatively straightforward to interpret and consisted of clear opaque and translucent zones. When compared to otoliths from bigeye tuna in the Indian Ocean, that were prepared using the same methods (Farley et al., 2021c), the yellowfin tuna sections were much easier to interpret even in otoliths from the largest fish (i.e., 78.8 cm FL). In yellowfin tuna, we did not observe the splitting or merging of zones or the increasing presence of diffuse black otolith material that was present in bigeye tuna otoliths, and even though the zones become more closely spaced near the otolith edge, they changed very little between the mid and outer areas of the section (Figure 5A and B).

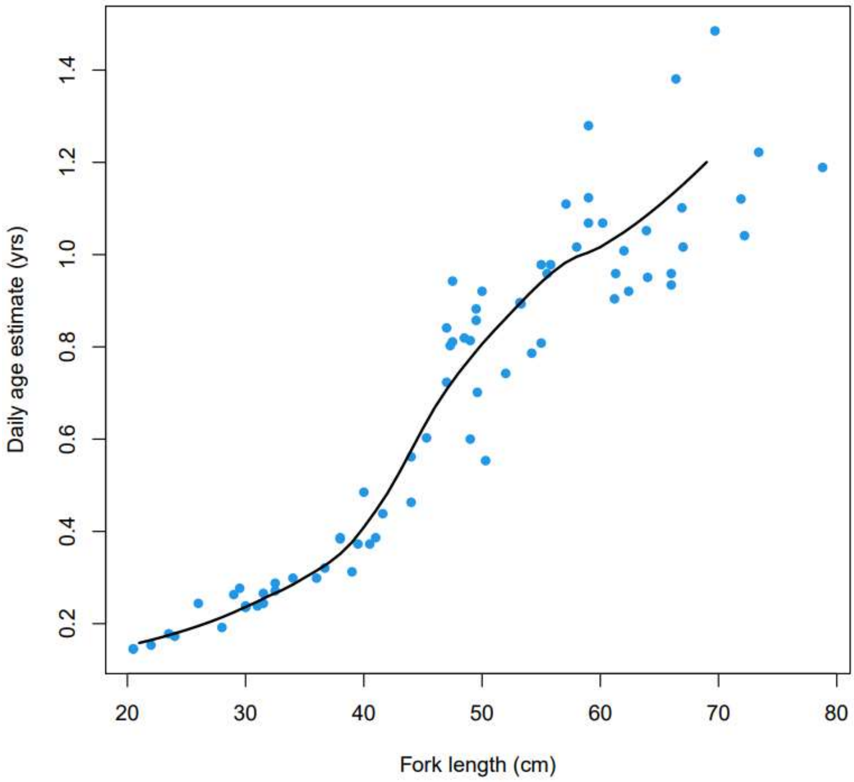

Figure 4. Relationship between fork length (FL) (cm) and daily age (microincrement count from longitudinal section) for yellowfin tuna, with a non-parametric smooth model fitted to the data using the loess function in R (R Core Team 2021). Note that only fish < 70 cm FL were included in the smooth since the data are too variable for larger fish for us to be confident in the age-length relationship.

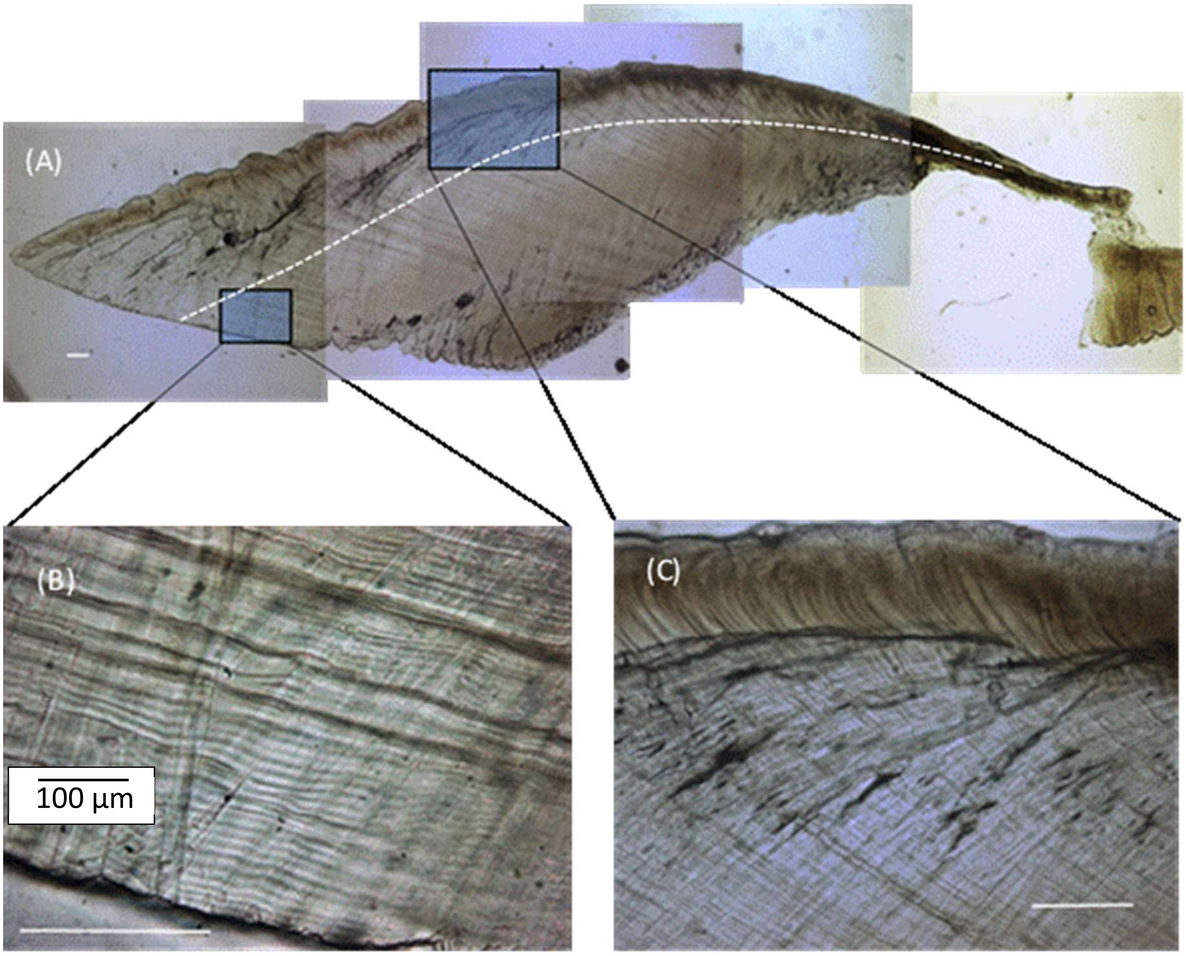

Figure 5. (A) Image of a yellowfin tuna otolith prepared as a longitudinal section for daily ageing showing magnified areas from the mid (B) and outer (C) areas of the section. Fish of 78.5 cm FL with a total estimated age 434 days. The white dotted line is the preferred counting path. Scale bar on all images is 100 µm.

Daily age estimates for the nine transverse sections re-read by FAS were lower than obtained by either Team 1 or Team 2 in the Sardenne et al. (2015) study (Figure 6). The FAS reader noted that interpreting the micro-structure was difficult and resulted in age estimates that were of low confidence. Differences in interpretation between readers could be due to two factors. First, readers in the Sardenne et al. (2015) may have been counting more zones in the initial part of the otolith. The prominent zones along the count path often consisted of a few smaller zones (see Figure 7). Along the initial count path that FAS use, the zone pattern is far more consistent and obvious. Secondly, the prepared sections by Sardenne et al. (2015) were reasonably thick (approx. 120 µm) compared to the thickness that FAS prepare otoliths for transverse daily ageing (approx. 60 µm). The reason otoliths are polished to a thin level is to reduce the risk of counting the same increment more than once due to the curvature of the increments.

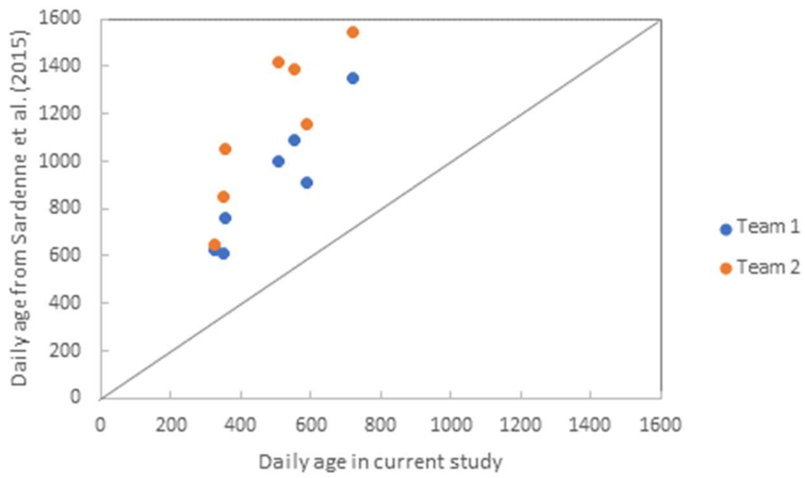

Figure 6. Comparison of daily age estimates for yellowfin tuna by FAS in the current study and by Team 1 and Team 2 in Sardenne et al. (2015).

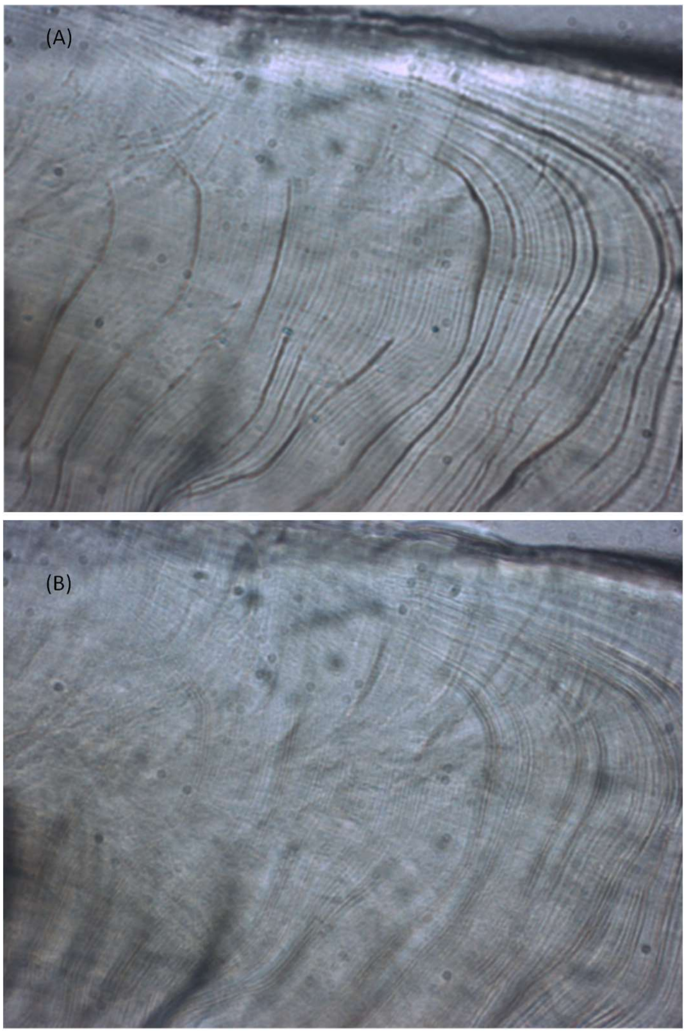

Figure 7. Two images of the same region within a transversely prepared yellowfin tuna otolith from Sardenne et al. (2015) magnified at 400x using two different focal distances. A) focus is on the surface (including the etched increments) and B) focus is on the increments under the surface.

3.2. Annual ageing

Counts of opaque zones were obtained for all 203 otoliths read for annual ageing. The counts ranged from 0 to 10 years. Figure 8 is an example of an otolith prepared for annual ageing with the (assumed) annual opaque zones marked. The intra-reader average percent error between readings was 3.8% with a maximum difference of 2 years (Table 1).

The relationship between fish length and otolith length on the counting path was close to linear (Figure 9), confirming that otoliths continue to growth throughout life and that increment widths are likely to be proportional to fish growth. Note that the age and otolith size of three fish did not correspond to the fork length and were removed from further analysis (<1 year but the fish lengths were 88, 141 and 157 cm FL), leaving 200 annual age estimates.

Decimal age was calculated for each fish based on the algorithm described in section 2.2 "Annual ageing". The calculated decimal ages ranged from 0.14 to 10.9 years. When daily and annual age estimates from the same fish were directly compared (n=24), the linear relationship was almost identical to the 1:1 line of agreement (Figure 10), indicating that the method to calculate decimal age from annual counts for these fish is working successfully. For fish with both a daily and annual age estimate, only the daily estimate was included in the growth analysis. Thus, 176 annual age estimates were included in the growth models (203 total – 3 outliers – 24 daily estimates). The relationship between otolith weight and age was curvilinear with a high goodness of fit (Figure 11), suggesting that otolith weight may be a good indicator of age, particularly for small/young fish.

Figure 8. Transverse preparation of a yellowfin tuna otolith prepared for annual reading showing presumed annual opaque zones indicated by white circles (n=10). Fish length 170 cm FL.

Table 1. Difference in age estimates between otolith readings by Fish Ageing Services (FAS) for yellowfin tuna.

Difference	Frequency	% Frequency
-2	1	0.5
-1	28	13.8
0	**155**	**76.3**
1	19	9.4
2	0	0
	203	100

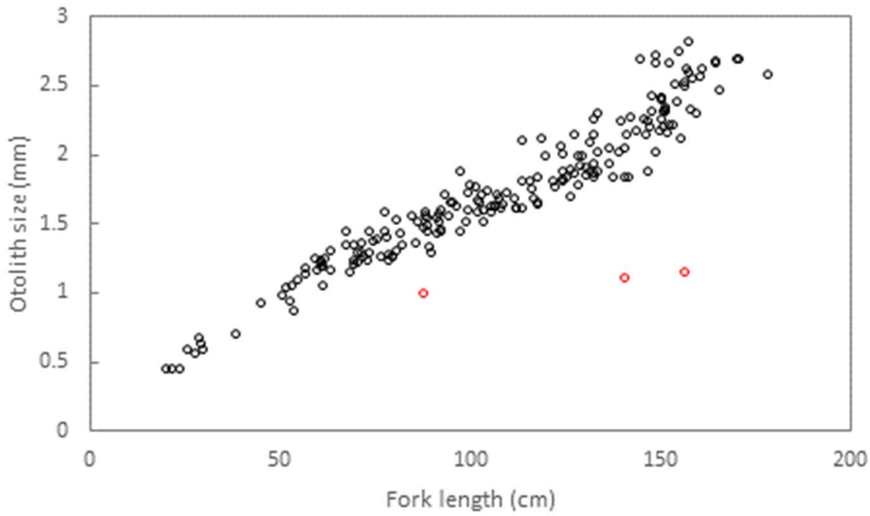

Figure 9. Relationship between fish length and otolith size (distance from the primordium along the counting path in transverse section) (n=203). Three clear outliers (red points) were removed from the growth analysis.

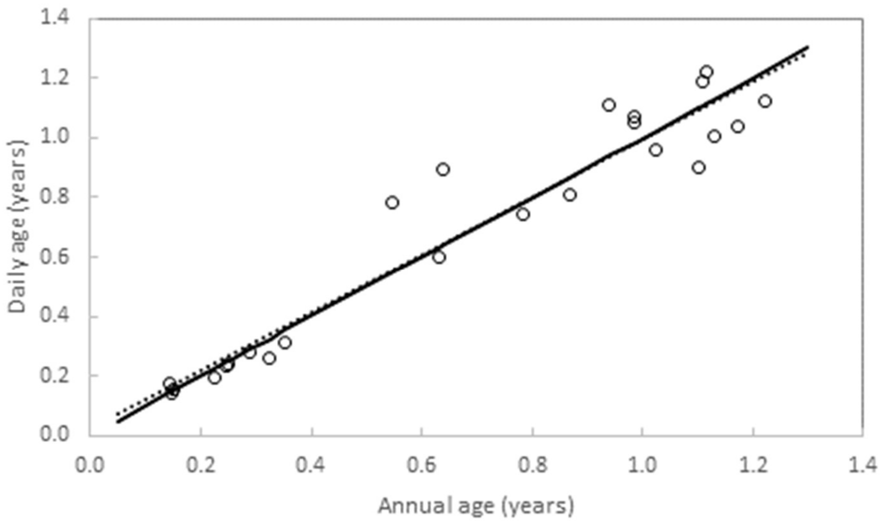

Figure 10. Comparison of daily and annual age estimates from sectioned otoliths sampled from the same fish (n=24). The 1:1 line is shown (solid black line) and the linear relationship between daily and annual age (dashed line; R^2 = 0.924).

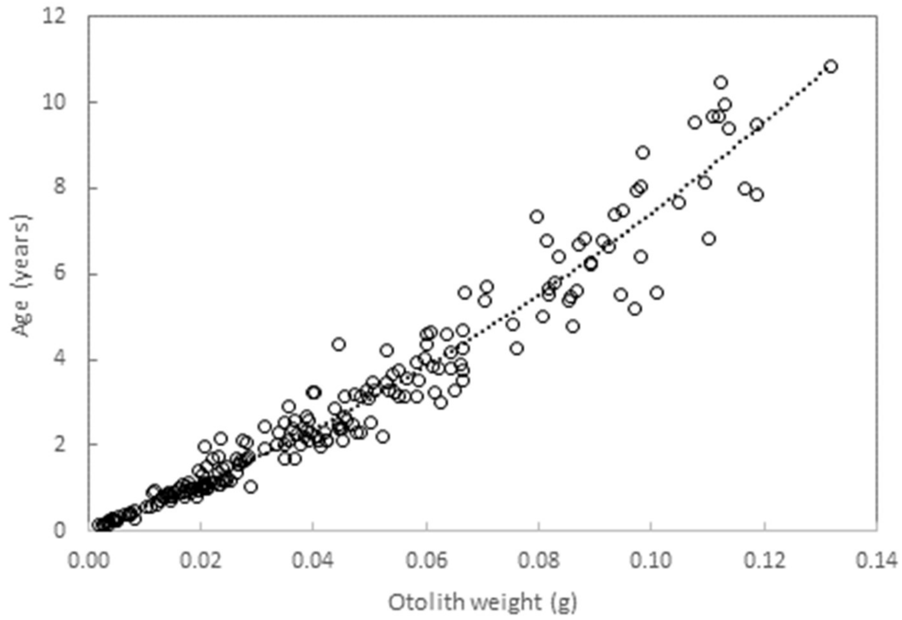

Figure 11. Relationship between otolith weight and estimated age (n=212). R^2 = 0.9496.

3.3. Age validation and verification

Analysis of IOTTP tag-recapture otoliths

Figure 12 shows the estimated age (daily and annual) of yellowfin tuna obtained in the current study against otolith size (transverse section). The same information for yellowfin tuna recaptured from the IOTTP, for which we have an otolith size estimate, is also included in Figure 12; for these individuals age at recapture was estimated from length at release and time at liberty (see Methods). The general consistency of the independent data sets for yellowfin tuna <age 8 years of age suggests that the otolith age estimates are accurate. As noted earlier, the time at liberty was known for each fish so a truly blind read was not possible at this time. Additional work will be undertaken on the OTC marked otoliths to evaluate whether the number of increments after the OTC mark is consistent with the time at liberty.

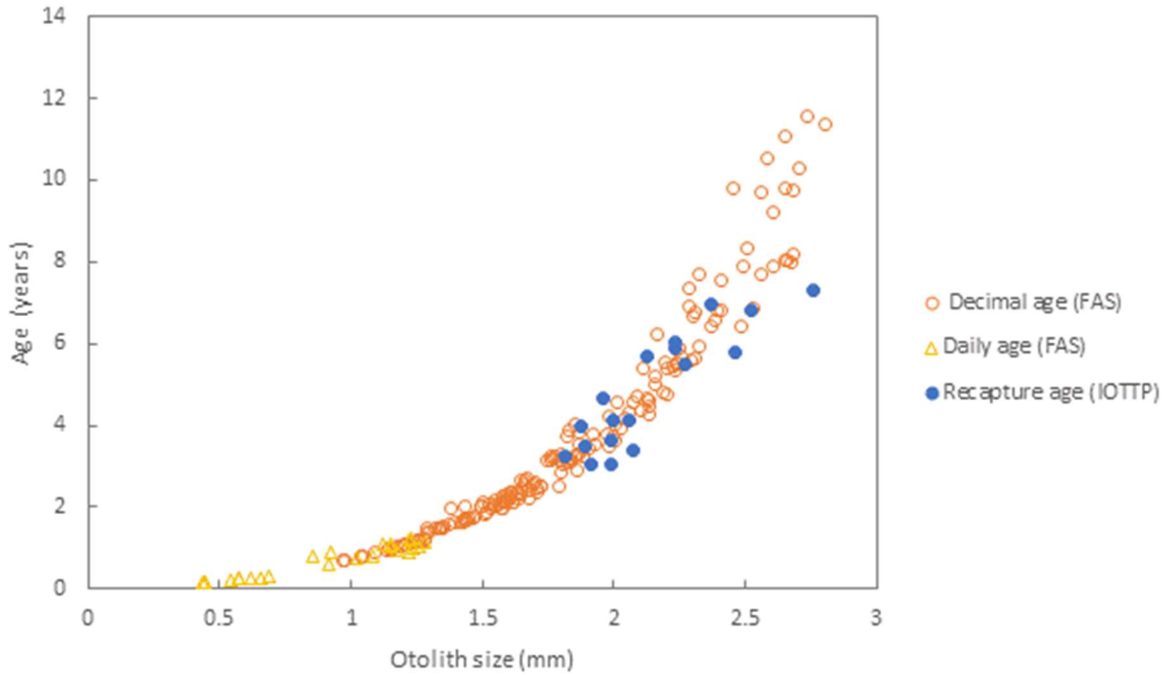

Figure 12. Otolith size versus age estimated by FAS (daily and decimal annual) for yellowfin tuna in this study as well as otolith size versus estimated recapture age of yellowfin tuna tagged and recaptured in the IOTTP for which otolith size was measured in the current study (n=18). Recapture age was estimated from release length and time at liberty (see Methods section 2.3). Otolith size is the distance from the primordium to the edge in transverse sectioned otoliths.

Analysis of IOTTP tag-recapture data

Figure 13 shows the length and age estimates for all yellowfin tuna aged in the current study as well as for yellowfin tuna recaptured in the IOTTP (in these cases age was estimated from release length and time at liberty). Although the tagging data suggests faster growth between 60-120 cm FL (see Discussion), the mean length at age is similar between these two independent data sets and provides further evidence that the otolith ageing method used in this project is accurate (i.e., unbiased). Unfortunately, the longest time at liberty for a tagged yellowfin was only 6.5 years, so this method can only help to verify age estimates up to ~7.5 years. However, the higher otolith age estimates obtained in the current study seems realistic since the otoliths were considerably heavier than the otoliths from fish aged 7-8 years (Figure 13).

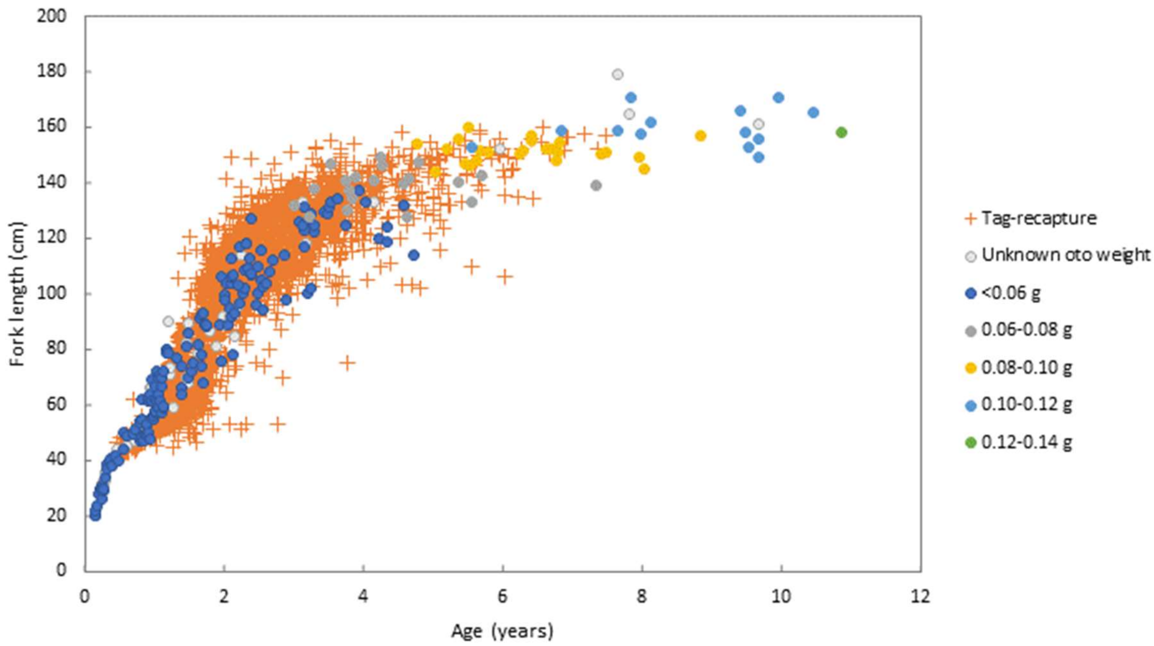

Figure 13. Age versus length data obtained in the current study shown by otolith weight bin (see key). Also shown is age versus length at recapture for yellowfin tuna tagged and recaptured in the IOTTP. Recapture age was estimated from release length and time at liberty (see Methods section 2.3).

3.4. Growth analysis

A total of 250 age-length data points were included in the growth models (176 decimal annual age estimates and 74 daily age estimates). The four growth models (VB, Richards, VB log k, and 2-stage VB) provide similar fits to the data (Figure 14; Append Figure 3), except the 2-stage VB model provides a better fit to small fish (< ~55 cm FL) (Figure 14B; Append Figure 3). Although the AIC value for the Richards model is smallest, the AIC for the 2-stage VB model is within 0.3 units (Table 2). The 2-stage VB model indicates there is a transition between two VB growth phases at age 0.83 years (53 cm FL), with a very high growth rate parameter in the first phase (k_1=2.9) followed by a lower growth rate parameter in the second phase (k_2=0.42) (Table 2).

Since otolith weight may be an indicator of age, we examined the otolith weight to fish length relationship of a larger number of samples (n=335) than were aged (n=250), to ascertain if the otolith growth was consistent with the observed fish growth. The results show a similar pattern in growth, with a transition at ~55 cm FL from a fast-growing phase to a slower-growing phase (Figure 15). This transition in otolith growth (and presumably fish growth) was not observed in yellowfin tuna otoliths from the WCPO (Figure 15), suggesting slightly different growth patterns for juvenile yellowfin tuna between these oceans. Overall, however, yellowfin tuna growth in the Indian Ocean and Western Pacific Ocean appears to be similar.

The length-at-age data were insufficient to model sex-specific or region-specific growth within the Indian Ocean. However, preliminary data exploration indicated that males may grow slightly faster and reach slightly larger sizes, on average, than females (Append Figure

4). This was supported by the length-at-otolith weight data for a larger number of samples (Append Figure 5). There is also some indication that juvenile yellowfin tuna between 55-80 cm FL (~age 1) in the NIO and NCIO regions have slightly larger length-at-age than yellowfin tuna in the other regions (Append Figure 6), but the sample size is too small to be conclusive and other factors such as size-selective fishing could bias the data. The length-at-otolith weight data were also consistent with this result but very few samples were available from the eastern Indian Ocean in the current project (Append Figure 7).

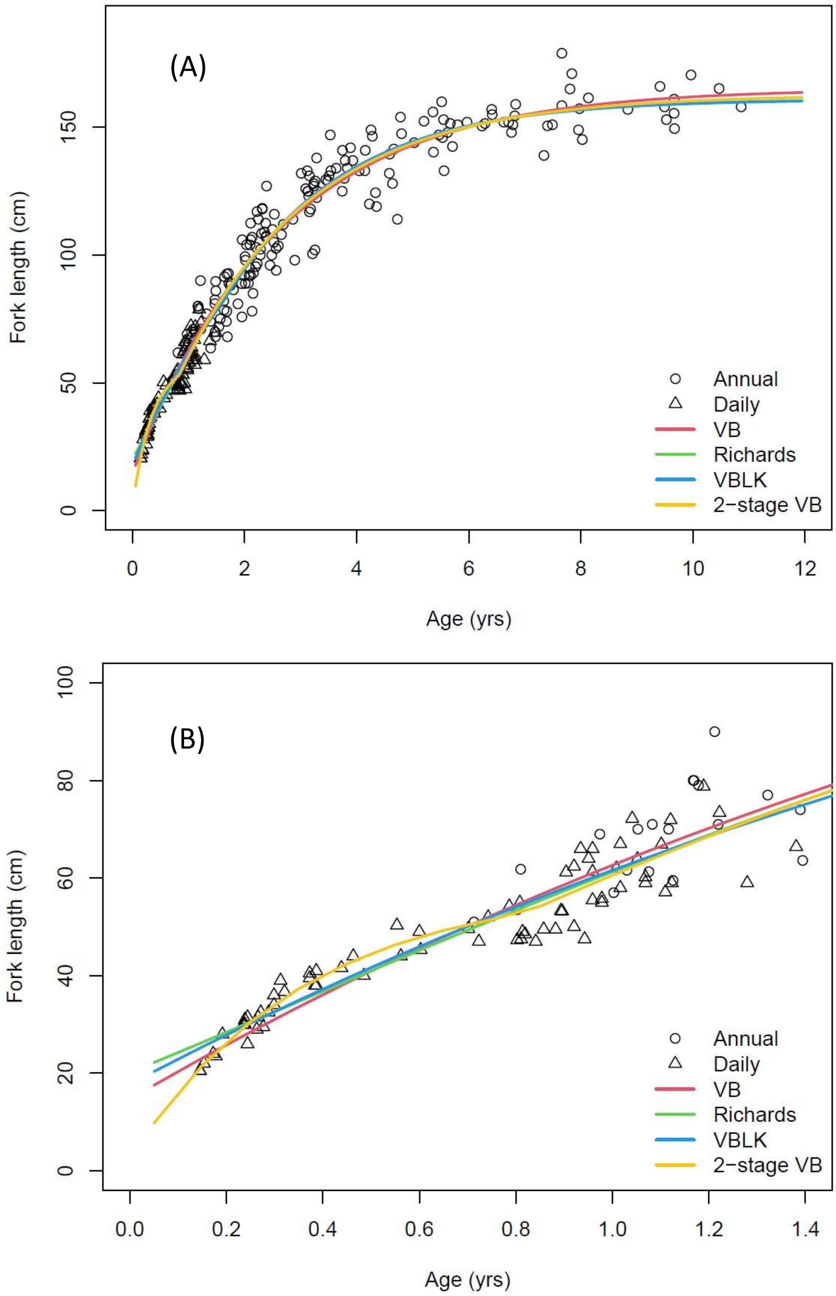

Figure 14. (A) Length-at-age data (daily and annual) for yellowfin tuna with von Bertalanffy (VB), Richards, VB log k (VBLK) and 2-stage VB growth models fit to the data. (B) A close-up of the length-at-age data and growth curves shown in (A) for small/young yellowfin tuna.

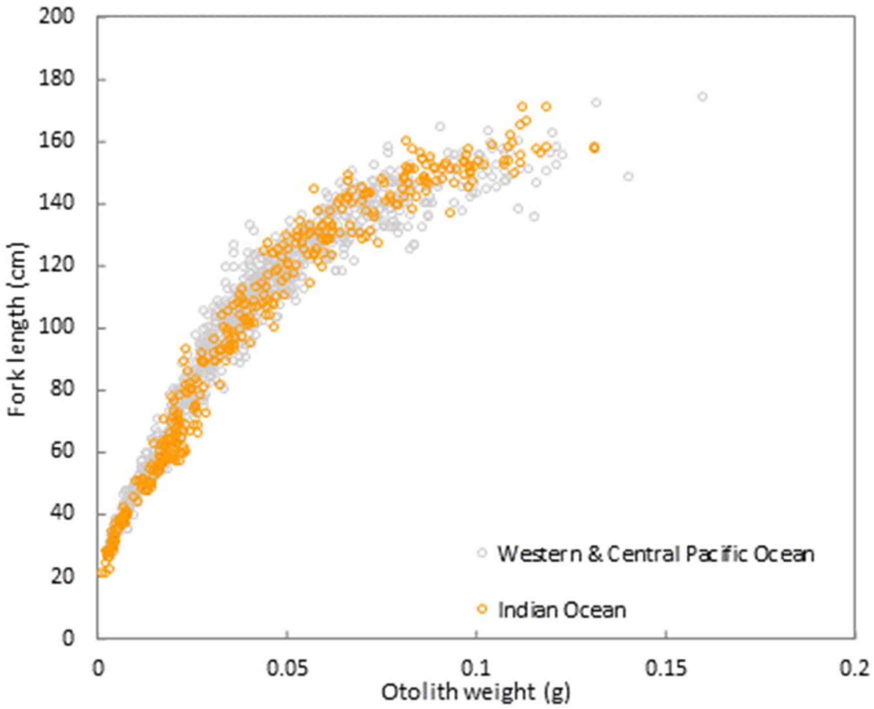

Figure 15. Relationship between otolith weight and fork length for yellowfin tuna in the Indian Ocean from the current study (i.e., GERUNDIO, EMOTION, PSTBS_IO and IOTTP projects) (n=335) and in the western and central Pacific Ocean from Farley et al. (2019; 2020) (n=991).

Table 2. Parameter estimates from fitting von Bertalanffy (VB), Richards, VB log k and 2-stage VB growth models to the yellowfin tuna length at age data (n=250). Standard errors for the parameter estimates are given in parentheses.

Model	L_∞	k/k_1	k_2	α	$b/\beta/\tau$	a_0/a^*	σ	AIC
VB	165.2 (1.9)	0.38 (0.01)	--	--	--	-0.24 (0.03)	8.07 (0.36)	1761.7
Richards	161.0 (2.2)	0.48 (0.05)	--	--	1.68 (0.51)	0.36 (0.22)	7.98 (0.36)	1757.9
VB log k	160.9 (2.2)	0.37 (0.02)	0.46 (0.04)	1.93 (0.31)	30* (NA)	-0.32 (0.06)	7.94 (0.36)	1759.7
2-stage VB	162.7 (2.0)	2.90 (1.3)	0.42 (0.02)	0.83 (0.09)	0.35 (0.03)	-0.01 (0.08)	7.92 (0.35)	1758.2

4. Discussion

This study applied recently developed methods to estimate a decimal age for yellowfin in the Indian Ocean from counts of annual growth zones in sectioned otoliths. The length-at-age data were combined with otolith-based daily age estimates from small fish to obtain age estimates for yellowfin tuna ranging from 20 to 179 cm FL. The annual and daily age estimates aligned well (see Figure 14), supporting our method to calculate the decimal age of yellowfin tuna. Preliminary age validation/verification work using otoliths and data from the IOTTP provide evidence that the otolith ageing method used in this study is accurate. However, we recommend that further age validation work is undertaken, including the analysis of bomb radiocarbon (^{14}C) data from otoliths (currently underway as part of the GERUNDIO project) and analysis of the OTC marked otoliths by a reader with no prior knowledge of the time at liberty or fish length.

The 2-stage VB model provided a better fit to the length at age data for fish < ~55 cm FL than the other three models considered. The length-at-otolith weight data (which is independent of the age estimation method) also showed changes in growth consistent with the length-at-age data, which lends support for the 2-stage VB growth model. Overall, our analysis shows that growth is rapid in the first few years with fish reaching ~60 cm FL at age 1 and ~95 cm FL at age 2. Mean asymptotic length was estimated to be ~163 cm FL and maximum age is at least 10.9 years.

The two-stage VB growth curve we estimated is quite different from the "ad hoc" growth curve of Fonteneau (2008) and VB log k growth curves of Eveson et al. (2015) and Dortel et al. (2015) (Figure 16), which, despite some variability between models, all suggest that growth in yellowfin tuna is slow between 30 and 60 cm FL (age 1 and 2 years) and then much faster between 60 and ~120 cm FL. The "ad hoc" growth curve of Fonteneau (2008) was estimated using growth increments in tag-recapture data from the IOTTP, and assumptions about how growth rates change outside the range of the tagging data. The Eveson et al. (2015) growth curves included tag-recapture data from the IOTTP and otolith-based daily age estimates from Sardenne et al. (2015). The tagging data were most influential in determining the shape of the curves; however, the otolith daily age data were useful for estimating the age of the tagged fish at release. The daily age data from Sardenne et al. (2015) varied considerably between two reader teams, and also between FAS and these two teams for the nine otoliths re-read in this study; this highlights that otolith structure can be interpreted differently by different readers. Eveson et al. (2015) estimated two growth curves, both using the same tag-recapture data but using daily age data from each reader team separately; this resulted in a shift of the curve along the age axis depending on which team's data were used but the shape of the curve and the mean asymptotic length was the same (130.7 cm FL). Dortel et al. (2015) estimated four growth curves: Model 1 used only the otolith daily age data from Sardenne et al. (2015); Model 2 used the otolith age data and modal progressions in length frequency data from the purse seine fishery; Models 3 and 4 used the otolith age and length frequency data as well as tag-recapture data from the IOTTP but with different distributions to model the ages at release. The growth curves by Dortel et al. (2015) were similar apart from mean asymptotic length, which was 165 cm, 155 cm, 139 cm and 138 cm FL for Models 1 to 4 respectively. Our 2-stage VB growth curve has a higher mean asymptotic length (~163 cm FL) compared to the growth curves that included tag-recapture data (130.7 cm FL in Eveson et al. (2015), and 139 and 138 cm FL for Models 2 and 3 in Dortel et al. (2015)). This may be due to the low number of fish >150 cm FL in the tag-recapture data available at the time for use in

Eveson et al. (2015) and Dortel et al. (2015), which is likely related to the relatively short times at liberty of fish included in the analysis (<6.5 years) compared to the estimated longevity of yellowfin tuna of at least 10 years.

Our 2-stage VB growth curve for yellowfin tuna is similar to growth estimated by Multifan-CL (MFCL) in the 2008 stock assessment (see Langley et al. 2008) for fish < ~90 cm FL (Figure 16). The divergence in growth for fish larger than 90 cm FL is not surprising since MFCL relies on length frequency data from catches to estimate growth parameters, which are imprecise when length modes merge across age classes as fish grows. Neither of these curves include tag-recapture data from the IOTTP.

The reason for the differences between growth curves reported amongst studies requires further investigation, but could be due to a number of factors. For the growth curves that include IOTTP tag-recapture data, there has been discussion about whether the two-stanza growth pattern observed in these data is am accurate reflection of growth of the population or due to factors including selectivity of fishing gear, environmental or genetic factors or tagging effects (Kolody 2011; Maunder et al. 2015). The release lengths of yellowfin tuna in the IOTTP had two very distinct modes separated around 55 cm FL; fish in the smaller length mode tended to have much slower growth rates than fish in the larger mode, which may suggest a tagging effect (see Eveson and Farley (2021) for further discussion). As for the differences between curves based on otolith age data, we know that interpretation of otolith increments is challenging and can differ substantially between readers and methods used. The daily age estimates obtained in the current study suggest a much different length-at-age than the daily age estimates derived from both reading teams in Sardenne et al. (2015) (Append Figure 8). The validation/ verification work we carried out using otolith size and weight data, and otoliths from the IOTTP tag-recapture study, indicate that both the daily and annual age readings obtained in this study are accurate (i.e., unbiased).

Figure 17 compares the otolith age and length data and estimated growth model for yellowfin tuna with the same information for bigeye tuna in the Indian Ocean (taken from Farley et al. (2021c)). Similarly, Figure 18 compares the otolith weight and fish length data for yellowfin tuna with the same data for bigeye tuna in the Indian Ocean (taken from Farley et al. (2021c)). Both datasets indicate that otolith growth is similar between species for fish up to ~60 cm FL, after which yellowfin growth is faster than bigeye growth before slowing rapidly and converging to a similar asymptotic length (~163 cm for yellowfin and 168 cm for bigeye).

We found some evidence that juvenile yellowfin tuna at around age 1 year in the NIO and NCIO regions may have slightly larger length-at-age than yellowfin tuna in the other examined in the Indian Ocean (Append Figure 6 andAppend Figure 7), which may suggest spatial structuring of yellowfin tuna in the Indian Ocean. The results are consistent with a recent genetic study by Grewe et al. (2021), which found evidence for genetic structure of Indian Ocean yellowfin tuna north and south of the equator. We recommend that additional otoliths are collected from the northern and eastern regions of the Indian Ocean where sample sizes are low, and that these otoliths and additional otoliths from those already collected in the GERUNDIO and IOTTP projects are read/aged to provide further information on growth and longevity. Sampling otoliths from fish of all length classes is recommended, and particularly fish > 100 cm FL in the norther regions. These data will also be useful for assessing the potential for inter-annual variation in length at age affecting estimation of the growth curve.

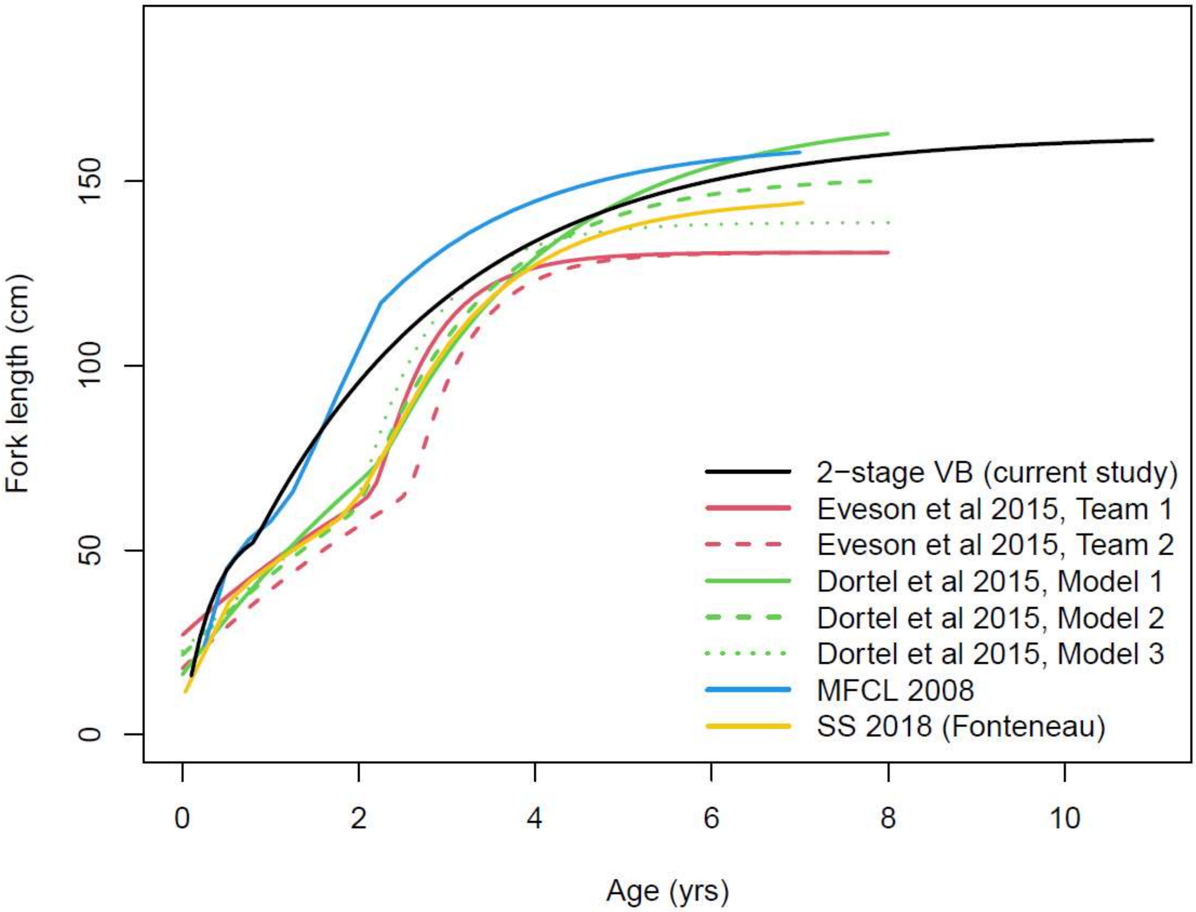

Figure 16. Comparison of the 2-stage VB growth curve estimated in the current study with growth curves estimated for Indian Ocean yellowfin tuna from other studies. VB = von Bertalanffy, MFCL = Multifan-CL, SS = Stock Synthesis.

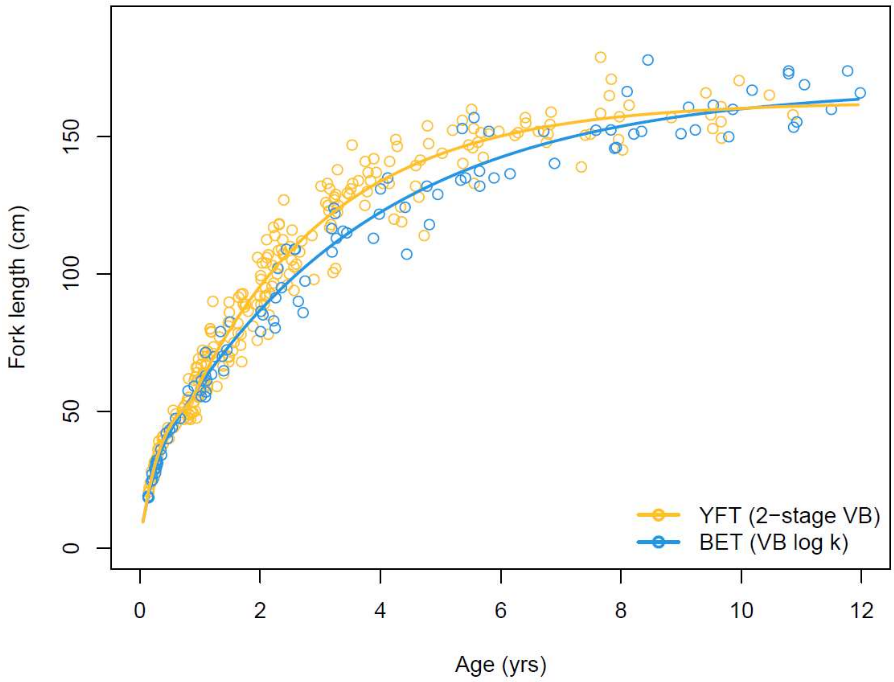

Figure 17. Comparison between Indian Ocean yellowfin and bigeye tuna age and length data, and estimated growth curves, from the current GERUNDIO study. Bigeye tuna information taken from Farley et al. (2021c).

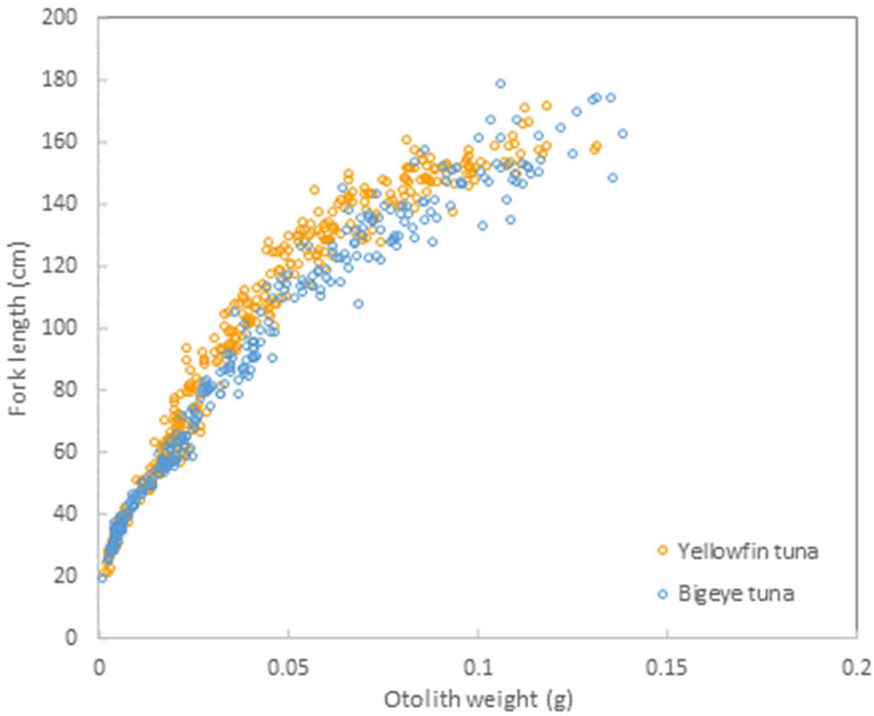

Figure 18. Relationship between otolith weight and fork length for yellowfin tuna (n=335) and bigeye tuna (n=352) in the Indian Ocean from the GERUNDIO study (i.e., samples collected under GERUNDIO, EMOTION, PSTBS_IO and IOTTP projects). The data for bigeye tuna was obtained from Farley et al. (2021c).

Acknowledgements

We are grateful to the many vessel skippers and crew involved in the project. We gratefully acknowledge all the observers, port samplers and coordinators for collecting, storing and transporting otoliths across the Indian Ocean. We want to thank Iñigo Krug and Iñigo Onandia (AZTI) who assisted in fish sampling and otolith extraction of those individuals collected from the Spanish cannery. We also thank Admir Sutrovic, Graham Porter and Christine Rees (FAS) for preparing and or weighing the otoliths. We thank the EMOTION (ANR 11 JSV7 007 01) and PSTBS-IO (GCP/INT/233/EC) projects for permitting the use of otoliths and data collected during the projects. The tuna tagging data analysed in this study were collected through the Indian Ocean Tuna Tagging Program (IOTTP) under the Regional Tuna Tagging Project of the Indian Ocean funded by the 9th European Development Fund (9.ACP.RSA.005/006) of the European Union, and small-scale tagging projects funded by the European Union and the Government of Japan, such as the West Sumatra Tuna Tagging Project. We wish to acknowledge the contributions of all the people that have been involved in the IOTTP and a special thanks to Fany Sardenne and Julien Barde (IRD) who kindly assisted with the transport of otoliths to CSIRO. The project is supported by financial assistance of the European Union (contract no. 2020/SEY/FIDTD/IOTC - CPA 345335). The views expressed herein can in no way be taken to reflect the official opinion of the European Union.

References

Akaike H (1974). A new look at the statistical model identification. IEEE Trans Autom Control 19: 716–723.

Andrews, A.H., Pacicco, A., Allman, R., Falterman, B.J., Lang, E.T., Golet, W. (2020). Age validation of yellowfin (*Thunnus albacares*) and bigeye (*Thunnus obesus*) tuna of the northwestern Atlantic Ocean. Canadian Journal of Fisheries and Aquatic Science 47: 637–643. dx.doi.org/10.1139/cjfas-2019-0328.

Anonymous (2002). A Manual for Age Determination of Southern Bluefin Thunnus maccoyii. Otolith Sampling, Preparation and Interpretation. Available at http://www.ccsbt.org/userfiles/file/docs_english/meetings/meeting_reports/ccsbt_09/report_of_daews.pdf/

Barth, J.M.I., Damerau, M., Matschiner, M., Jentoft, S., Hanel, R. (2017). Genomic Differentiation and Demographic Histories of Atlantic and Indo-Pacific Yellowfin Tuna (*Thunnus albacares*) populations. Genome Biol. Evol. 9: 1084–1098.

Beamish, R.J. and Fournier, D.A. (1981). A method for comparing the precision of a set of age determinations. Canadian Journal of Fisheries and Aquatic Sciences 38: 982–983. doi: 10.1139/f81-132.

Bodin, N., Chassot, M., Sardenne, F., Zudaire, I., Grande, M., Dhurmeea, Z., Murua, H., Barde, J. (2018). Ecological data for western Indian Ocean tuna. Ecology 99 (5) 1245-1245.

Collette, B.B., Reeb, C., Block, B.A. (2001). Systematics of the tunas and mackerels (Scombridae). Fish Physiol. 19 : 1–33. https://doi.org/10.1016/S1546-5098(01)19002-3.

Davies, C., Marsac, F., Murua, H., Fahmi, Z., Fraile, I. (2020). Summary of population structure of IOTC species from PSTBS-IO project and recommended priorities for future work. IOTC-2020-SC23-11_Rev1, 16p.

Dortel, E., Sardenne, F., Bousquet, N., Rivot, E., Million, J., Le Croizier, G., Chassot, E. (2015). An integrated Bayesian modeling approach for the growth of Indian Ocean yellowfin tuna. Fish. Res. 163, 69–84. https://doi.org/10.1016/j.fishres.2014.07.006.

Eveson, P., Farley, J. (2021). Investigating growth information for yellowfin and bigeye tuna from the IOTTP tag-recapture data. IOTC-2021-WPTT23-21.

Eveson, P., Million, J., Sardenne, F., Le Croizier, G. (2012). Updated growth estimates for skipjack, yellowfin and bigeye tuna in the Indian Ocean using the most recent tag-recapture and otolith data. IOTC-2012-WPTT14-23.

Eveson, P., Million, J., Sardenne, F., Le Croizier, G. (2015). Estimating growth of tropical tunas in the Indian Ocean using tag-recapture data and otolith-based age estimates. Fisheries Research 163: 58–68.

Farley, J., Eveson, P., Krusic-Golub, K., Sanchez, C., Roupsard, F., McKechnie, S., Nicol, S., Leroy, B., Smith, N., Chang, S.-K. (2017). Project 35: Age, growth and maturity of bigeye tuna in the western and central Pacific Ocean. WCPFC-SC13-2017/ SA-WP-01.

Farley, J., Krusic-Golub, K., Eveson, P. Clear, N., Luque, P. et al. (2021c). Estimating the age and growth of bigeye tuna (Thunnus obesus) in the Indian Ocean from counts of daily and annual increments in otoliths. IOTC-2021-WPTT23-18.

Farley, J., Krusic-Golub, K., Eveson, P., Clear, N., Rouspard, F., Sanchez, C., Nicol, S., and Hampton, J. (2020). Age and growth of yellowfin and bigeye tuna in the western and central Pacific Ocean from otoliths. WCPFC-SC16-2020/SC16-SA-WP-02.

FAO (2020). The State of World Fisheries and Aquaculture 2020 – Sustainability in Action. FAO, Rome.

Fonteneau, A. (2008). A working proposal for a Yellowfin growth curve to be used during the 2008 yellowfin stock assessment. IOTC-2008-WPTT-4.

Fu, D. Langley, A. Merino, G. Urtizberea, U. (2018). Preliminary Indian Ocean yellowfin tuna stock assessment 1950-2017 (stock synthesis). IOTC–2018–WPTT20–33

Grewe, P, Feutry, P, Foster, S, Aulich, J, Lansdell, M, et al. (2020). Genetic population connectivity of yellowfin tuna in the Indian Ocean from the PSTBS-IO Project. IOTC-2020-WPTT22(AS)12_REV1.

Guillotreau, P., Squires, D., Sun, J., Compeán, G.A. (2017). Local, regional and global markets: what drives the tuna fisheries? Rev. Fish Biol. Fisheries 27:909–929

Hearn, W.S., Polacheck, T. (2003). Estimating long-term growth-rate changes of southern bluefin tuna (*Thunnus maccoyii*) from two periods of tag-return data. Fish. Bull. 101:58-74.

IOTC (2020). Report of the 22nd Session of the IOTC Working Party on Tropical Tunas, Stock Assessment Meeting. OTC–2020–WPTT22(AS)–R[E]_Rev1.

Ishihara, T., Abe O., Shimose, T., Takeuchi, Y., Aires-da-Silva, A., (2017) Use of post-bomb radiocarbon dating to validate estimated ages of Pacific bluefin tuna, *Thunnus orientalis*, of the North Pacific Ocean. Fisheries Research, 189: 35-41.

Kunal S.P., Kumar G., Menezes M.R., Meena R.M. (2013). Mitochondrial DNA analysis reveals three stocks of yellowfin tuna *Thunnus albacares* (Bonnaterre, 1788) in Indian waters. Conserv Genet. 14: 205–213.

Kolody, D. (2011). Can length-based selectivity explain the two stage growth curve observed in Indian Ocean YFT and BET? OTC–2011–WPTT13–33.

Langley, A., Hampton, J., Herrera, M., Million, J. (2008). Preliminary stock assessment of yellowfin tuna in the Indian Ocean using MULTIFAN-CL. IOTC-2008-WPTT-10.

Laslett, G.M., Eveson, J.P., Polacheck, T. (2002). A flexible maximum likelihood approach for fitting growth curves to tag-recapture data. Can. J. Fish. Aquat. Sci. 59, 976–986.

Maunder, M.N., Crone, P.R., Valero, J.L., Semmens, B.X. (2015). Growth: theory, estimation, and application in fishery stock assessment models CAPAM Workshop Series Report 2 March 2015.

Maunder, M.N. Piner, K.R. (2015). Contemporary fisheries stock assessment: many issues still remain. ICES J. Mar. Sci. 72 (1): 7-18.

McKinney, R., Gibbon, J., Wozniak, E., Galland, G. (2020). Netting billions 2020: A global tuna valuation. The Pew Charitable Trusts.

Methot, R.D., Wetzel, C. (2013). Stock Synthesis: a biological and statistical framework for fish stock assessment and fishery management. Fish. Res. 142: 86-99.

Murua, H., Eveson, J.P., Marsac, F. (2015). The Indian Ocean Tuna Tagging Programme: Building better science for more sustainability. Fish. Res. 163:1-6.

Murua, H., Rodrıguez-Marin, E., Neilson, J., Farley, J., Juan-Jorda, M.J. (2017) Fast versus slow growing tuna species – age, growth, and implications for population dynamics and fisheries management. Rev. Fish Biol. 27: 733-773. DOI 10.1007/s11160-017-9474-1.

R Core Team (2021). R: A language and environment for statistical computing. R Foundation for Statistical Computing, Vienna, Austria. URL https://www.R-project.org/.

Reglero, P., Tittensor, D., Ά lvarez-Berastegui, D., Aparicio-González, A., Worm, B. (2014). Worldwide distributions of tuna larvae: revisiting hypotheses on environmental requirements for spawning habitats. Mar. Ecol. Prog. Ser. 501, 207–224. https://doi.org/10.3354/meps10666.

Richards, F.J. (1959). A flexible growth function for empirical use. J. Exp. Bot. 10(2): 290-301.

Sardenne, F., Dortel, E., Le Croizier, G., Million, J., Labonne, M., Leroy, B., Bodin, N., Chassot, E. (2015) Determining the age of tropical tunas in the Indian Ocean from otolith microstructures. Fish. Res. 163:44–57. doi:10.1016/j.fishres.2014.03.008.

Schaefer, K.M. (2001). Reproductive biology of tunas. *In:* Block, B.A., Stevens, E. (Eds.), Tuna: Physiology, Ecology and Evolution. Academic Press, San Diego, California, pp. 225–270, https://doi.org/10.1016/S1546-5098(01)19007-2.

von Bertalanffy, L (1938). A quantitative theory of organic growth (inquiries on growth laws. II). Human Biol 10: 181–213.

Williams, A.J., Leroy, B.M., Nicol, S.J., Farley, J.H., Clear, N.P., Krusic-Golub, K., Davies, C.R, (2013) Comparison of daily- and annual- increment counts in otoliths of bigeye (*Thunnus obesus*), yellowfin (*T. albacares*), southern bluefin (*T. maccoyii*) and albacore (*T. alalunga*) tuna. ICES J. Mar Sci 70(7): 1439–1450. doi:10.1093/icesjms/fst093.

Appendix A – Otolith data for age algorithm

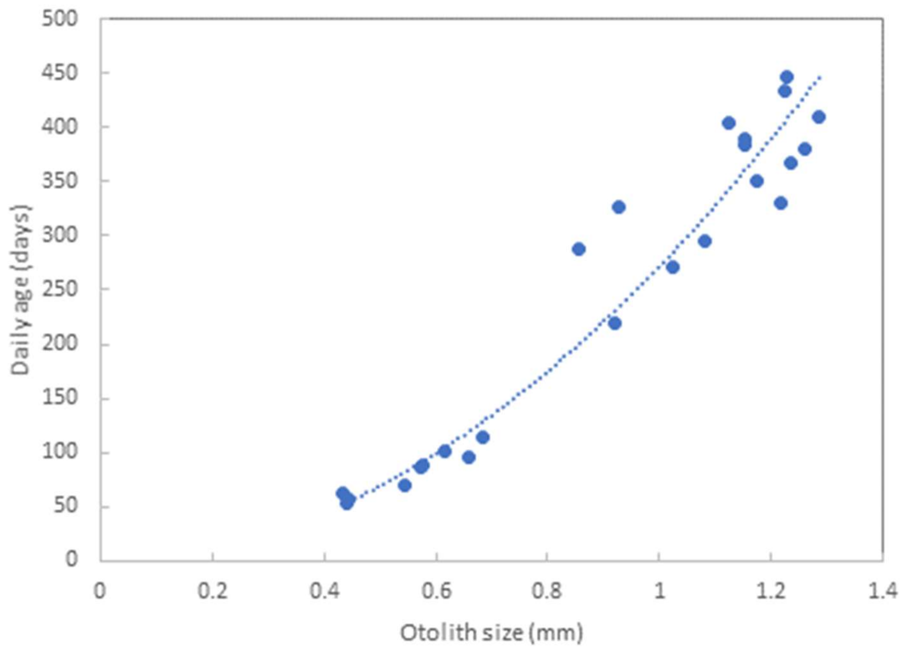

Append Figure 1. Relationship between daily age and otolith size with fitted power curve for yellowfin tuna. Otolith size is the distance from the primordium to the edge in transverse sectioned otoliths. R^2 = 0.9617.

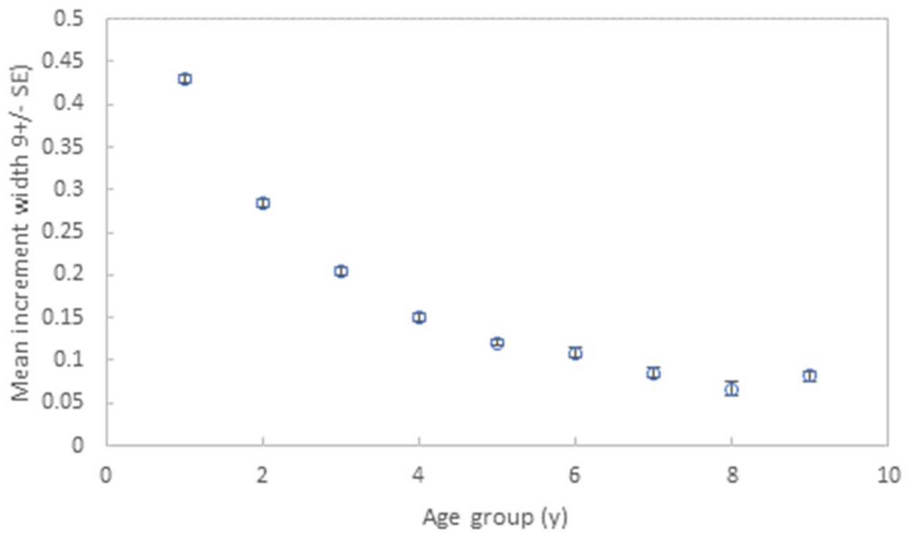

Append Figure 2. Mean (+/- SE) annual increment width in millimetres by age class for yellowfin tuna.

Appendix B – Diagnostic residual plots

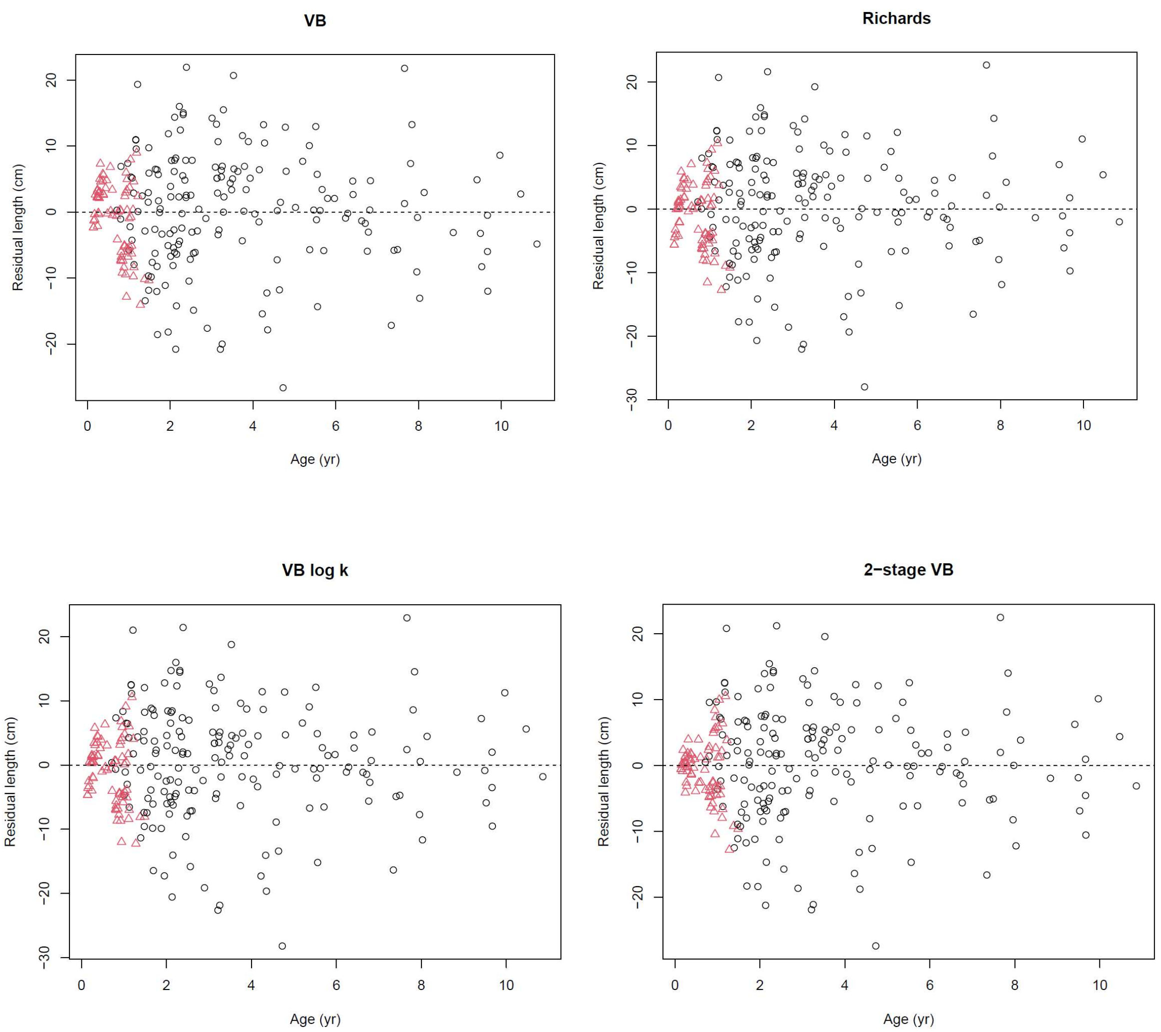

Append Figure 3. Diagnostic residual plots for the fit of the VB, Richards, VB log k and 2-stage VB growth models to the length at age data.

Appendix C – Growth by sex and region

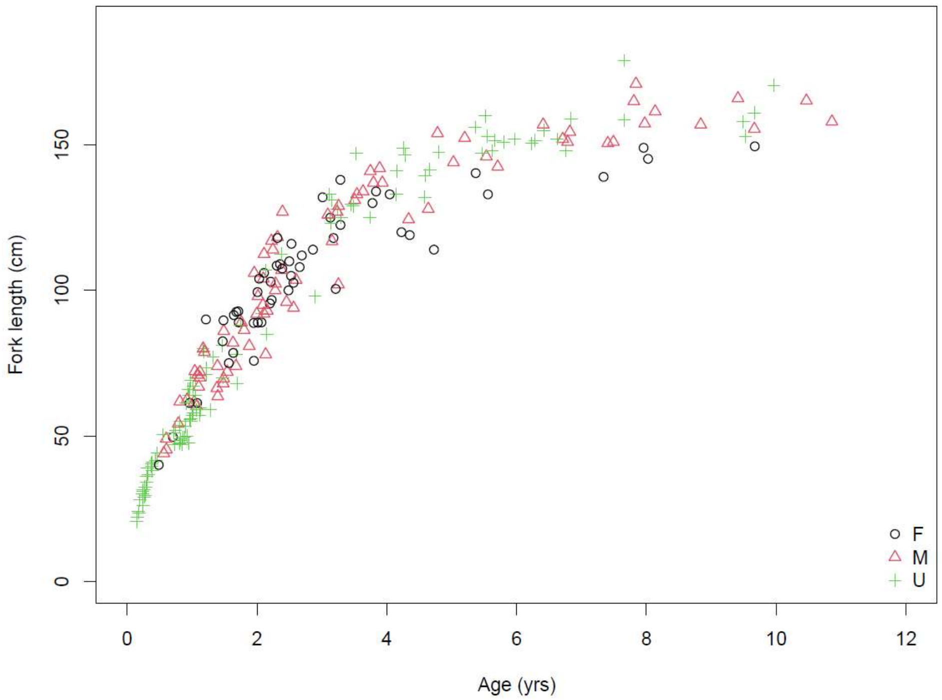

Append Figure 4. Length-at-age data for yellowfin tuna in the Indian Ocean by sex. There is some indication that males may grow slightly faster and reach slightly larger sizes, on average, than females.

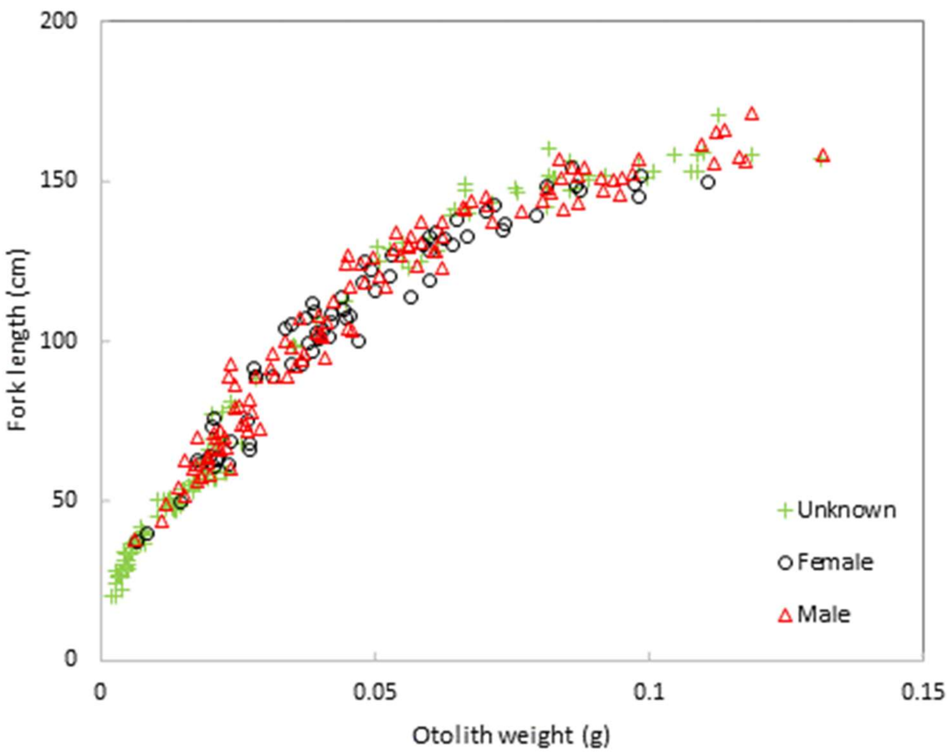

Append Figure 5. Relationship between otolith weight and fork length for yellowfin tuna in the Indian Ocean by sex. N=236.

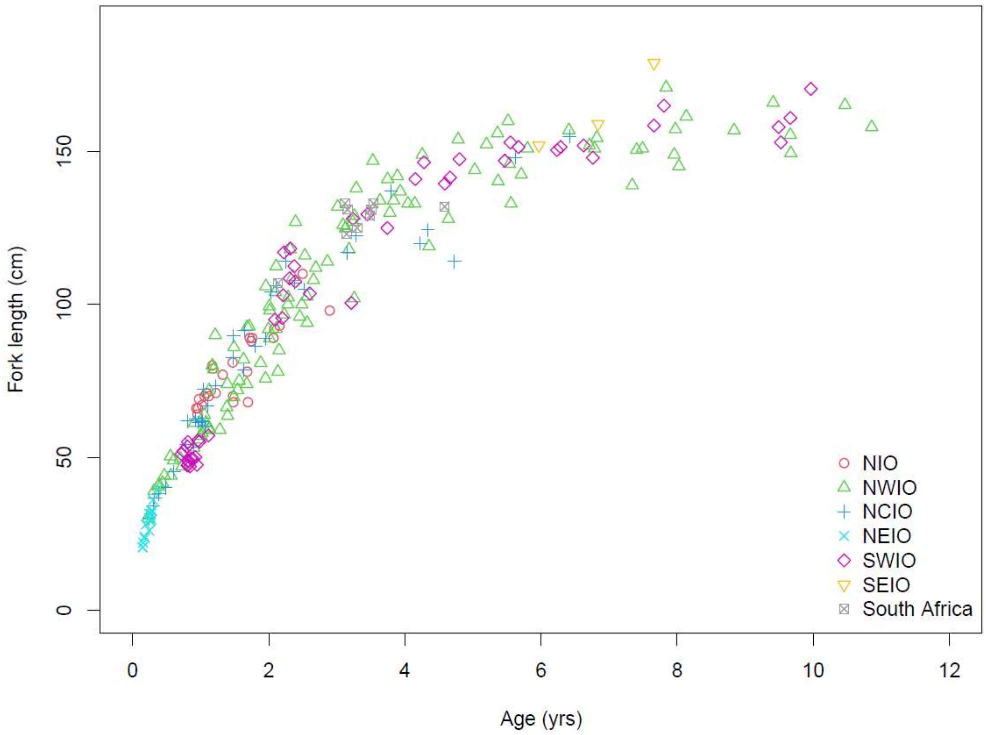

Append Figure 6: Length-at-age data for yellowfin tuna caught by region in the Indian Ocean. See Figure 1 for regions.

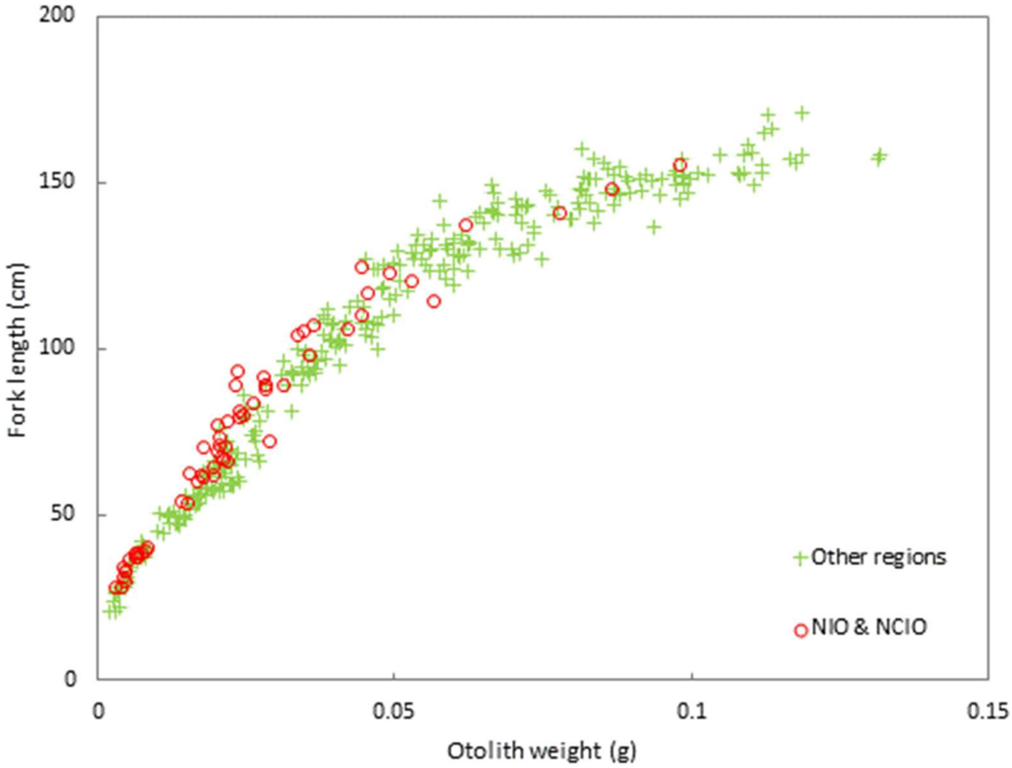

Append Figure 7. Relationship between otolith weight and fork length for yellowfin tuna caught in the North Indian Ocean (NIO) and North Central Indian Ocean (NCIO) combined and all other regions. See Figure 1 for regions. N=302.

Appendix D – Comparison of age estimates

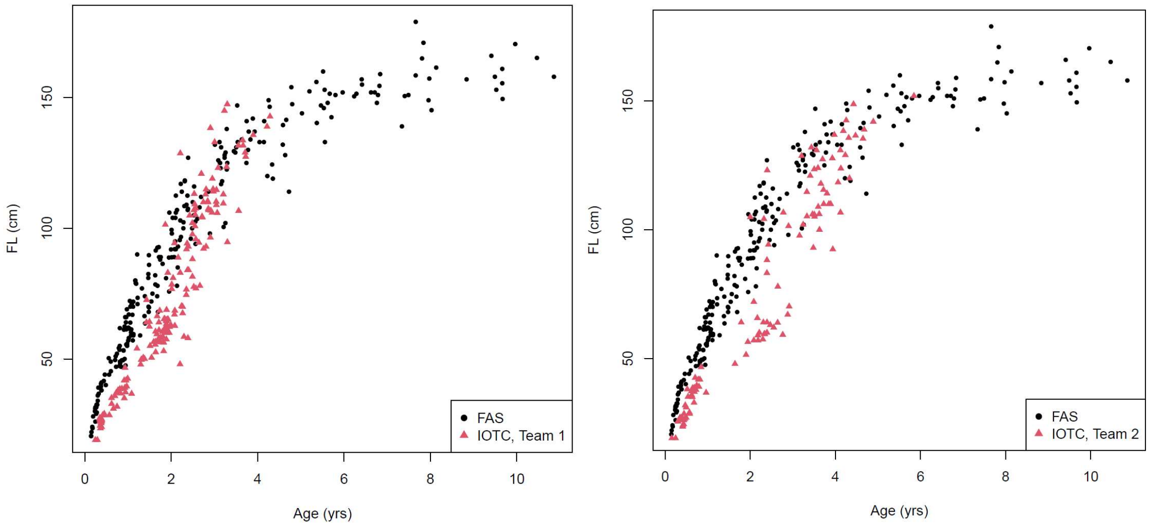

Append Figure 8. Comparison of age estimates obtained in the current study and daily age estimates obtained by reading Team 1 and Team 2 in Sardenne et al. (2015).